# Addressing Reviewer comments for "Modeling the Diurnal Variability of Agricultural Ammonia in Bakersfield, California during the CalNex Campaign"

We thank both reviewers for their helpful comments and suggestions. We provide specific responses to their comments below that coincide with changes, additions and corrections made in the paper. We feel this has resulted in an improved manuscript. Below reviewer comments are in italics while our responses are in normal typeface.

## Reviewer #1

*1) General comments: The authors present a NH3 modelling study based on a variety of ammonia measurements (surface, flight, satellite) performed during the CalNex measurement campaign. The focus lies on determining possible causes for the discrepancies in the diurnal variation between the modelled and observed concentrations. The paper further describes a few possible adjustments by applying a more representative temporal allocation of the NH3 emissions and the application of a bi-directional NH3 flux scheme. An interesting study is presented, comparing modelled concentrations with NH3 observations covering a range of the vertical and spatial distribution of ammonia concentrations. Potentially this could be a really useful and informative publication, as almost no model studies using this range of observations are available, but some work will be needed to improve it before final publication*

*In particular, I found that with the wealth of data and observations available more could be done, specifically on the presentation of the results and a systematic (final) discussion, which is more or less missing. The setup of the paper is done rather well, describing the observations used as well as the applied models etc. The results & discussion/conclusion section however will need some work. As an example the last section feels a bit rushed. In the first paragraph of the results the comparison is described in a systematic fashion, while for the final version of the model only a short description is given, lacking any final conclusions, which leaves the reader without any sense of improvement/idea that the final version of the model improved much but the bias (a bit).*

We thank the reviewer and agree with their comment. In order to address this concern we have rearranged the model results section so as to organize the paper around the three measurement platforms (ground, flight and satellite measurements) rather than around the different model sensitivity studies and added a new Discussion Section. Section 4.1 in the new manuscript evaluates a full month of output from the three different model scenarios, $CMAQ_{base}$, $CMAQ_B$ (bidirectional ammonia) and $CMAQ_{AB}$ (bidirectional and adjusted emissions), with the surface measurements. We thoroughly discuss the evaluation of the diurnal distributions of $NH_x$, $NH_{3(g)}$ and $NH_{4(p)}$ in the three scenarios, since the surface measurements provide the best available information for identifying diurnal patterns. Section 4.2 discusses the aircraft measurement comparisons as well as the vertical profile of $NH_x$, since the aircraft measurements provide insight into the vertical dispersion of $NH_x$ as well as the overall magnitude of emissions in the afternoon and evening hours Section 4.3 discusses the comparison of the three scenarios with the TES retrievals, including an added level-by-level comparison of the modeled and retrieved vertical profiles of $NH_3$. Section 5 then describes the remaining errors in the final model version ($CMAQ_{AB}$) and suggests possible explanations for these errors and directions for future research. The revised Conclusions Section (Section 6) summarizes the results and discussion, and now includes a description of the overall model bias changes as well as suggestions for future work on $NH_3$ modeling in the SJV.

*2) I am missing an overall figure with the observed and modelled concentrations for the Bakersfield concentrations. The authors do show the diurnal cycles and a boxplot for the individual hours but this does not give a feel of the possible events and variability between the days, which can occur during the measurement interval. A simple plot with the time series would bring some clarity. One could also add the observed TES observations as a second Y-axis. Another idea would be to add temperature/wind speeds to explain the variation of the concentrations (as emissions from fields for example are related to both).*

We have added a detailed time series plot (Figure 2 in the revised manuscript) that compares a full month of model output from our three model scenarios to ground measurements for $NH_x$, $NH_{3(g)}$, $NH_{4(p)}$, temperature, and wind speed. As the TES measurements are not directly comparable with the surface data we have not plotted them in Figure 2, but we feel that the additional figure (Figure 8 in the revised manuscript) and table (Table 3 of the revised manuscript) that we have added give additional context for the TES observations (see the response in comment 5 below). We also include a final model ($CMAQ_{AB}$) to measurement comparison in Figure 9 and discuss these results in the new Discussion Section (Section 5).

*3) On the measurements itself:*
*Surface: If the instruments used have an inlet with some piping etc, this could cause artifacts in the observed NH3 concentrations in the early morning. Some words on this and other possible artifacts would be helpful.*

We added Page 6, lines 12-17 (quoted below) to discuss how the measurement techniques address artifacts from inlets and other surface measurement uncertainties due to instrumentation and include an additional reference (Markovic et al., 2014).

> “At the Bakersfield ground site the Ambient Ion Monitor Ion Chromatograph (AIM-IC, Ellis et al., 2010, Markovic et al., 2012) was used to measure $NH_{3(g)}$ on an hourly basis, with an uncertainty of +/- 20 % and a detection limit of 41 ppt. The sampling inlet for the AIM-IC consists of an enclosure mounted at 4.5 m above ground, including a virtual impactor, parallel plate denuder, and particle supersaturation chamber, connected to the ion chromatography systems via several 20 m perfluoroalkyl sampling lines carrying the dissolved analytes (Markovic et al., 2014). This design reduces artifacts by minimizing the inlet surface area prior to scrubbing the $NH_3$ from the gas phase in the denuder, and by separating the gas and particle

> phase constituents while the sample flow is still at ambient temperature and relative humidity (Markovic et al., 2012)."

*4) Only seven days of the observations are used and compared with the model, is this the entire measurement period? If not why are only 7 days of the measurements used?*

Our original paper only covered a 7-day case study and we felt that a longer time period would provide a better evaluation. We have thus significantly expanded our three model scenarios to cover the entire month-long period of ground measurements at the Bakersfield supersite and added extensive discussion of these results to the paper. Page 9, lines 30-31 and Page 10, lines 1-5, in Section 4 describe the full range of model runs as follows:

> "In order to evaluate CMAQ v5.0.2 modelled $NH_3$ in the SJV we ran three different scenarios for a month long case-study that covers the record of the Bakersfield surface observations (May 22 – June 22, 2010). The model scenarios include: 1) a baseline model run ($CMAQ_{base}$), in which the model was set up as described in Section 3.2, utilizing the CARB emissions inventory; 2) $CMAQ_B$, which ran with the baseline set up but also included the bi-directional $NH_3$ scheme described in Section 3.2, and finally 3) $CMAQ_{AB}$, which included both the bi-directional $NH_3$ scheme and diurnally-varying emissions in the SJV, as described in Section 4.1. The following subsections describe the evaluations of all three model scenarios using the three different measurement datasets (surface, aircraft, and satellite) from the CalNex campaign."

We decided against re-running our sensitivity studies ($CMAQ_B$ and $CMAQ_{AB}$) to start at the initial model start of May 5th as we felt that a full month of comparison to ground measurements was sufficient to evaluate the two additional model scenarios ($CMAQ_B$ and $CMAQ_{AB}$) while minimizing the additional computational expense this would have caused. This time frame also included the majority of flight days and TES overpasses, and the average bias relative to TES for $CMAQ_{base}$ did not change significantly when excluding the two overpasses prior to May 22. We still present the comparisons of the $CMAQ_{base}$ model run with the two flights and TES overpasses prior to May 22nd in the Supplemental Material (Table S1 and S3).

*5) Satellite: I am not convinced by the model vs satellite comparison. Especially the comparison for the observations near Bakersfield look rather poor. Some words on the quality of the TES data? Also by using the RVMR on has to know for certain the vertical is described well in the model. The RVMR is only 20%-60% of the surface value, and depending on the NH3 profile doesn't have to be in relation to the surface. Some words on any effects caused by the RVMR and maybe a comparison on the profile of TES and the model? Similar to the study by shephard et al?: Shephard, M. W., McLinden, C. A., Cady-Pereira, K. E., Luo, M., Moussa, S. G., Leithead, A., Liggio, J., Staebler, R. M., Akingunola, A., Makar, P., Lehr, P.,* *Zhang, J., Henze, D. K., Millet, D. B., Bash, J. O., Zhu, L., Wells, K. C., Capps, S. L., Chaliyakunnel, S., Gordon, M., Hayden, K., Brook, J. R., Wolde, M., and Li, S.-M.: Tropospheric Emission Spectrometer (TES) satellite observations of ammonia, methanol, formic acid, and carbon monoxide over the Canadian oil sands: validation and model evaluation, Atmos. Meas. Tech., 8, 5189-5211, doi:10.5194/amt-8-5189-2015, 2015. Also the observed concentrations near Bakersfield seem to be quite low at time. Any effects due to the sensitivity/retrieval of TES for these low retrieved concentrations? You could add a figure with the observed and modelled profiles and the AVK of the satellite observations to show the difference in the vertical (and yes the DOF are low but the profiles are still used for the RVMR).*

We have added an additional figure (Figure 8) that follows a similar evaluation performed in Shephard et al. (2015, now included as a reference) and have included additional discussion of the satellite analysis (Section 4.3). The bias in the $CMAQ_B$ and $CMAQ_{AB}$ results relative to the TES RVMR has also been added as Table 3. The added discussion based on the new Figure 8 is as follows (Page 13, lines 25-33):

> "However, the model RVMR can be very sensitive to errors in the modelled vertical distribution of $NH_3$. We investigated this by comparing each level of the TES retrieved $NH_3$ profile with the corresponding CMAQ profile level after the observation operator is applied. Figure 8 shows box-and-whisker plots of this comparison for the $CMAQ_{base}$ and $CMAQ_{AB}$ model scenarios. This plot differs from that in Shephard et al. (2015) in that it includes the average of layers below 908 mb, which introduce an RVMR bias due to levels that are below 1000 mb. For $CMAQ_{base}$, there is a substantial negative bias in the lowest level (-5 ppb), but for $CMAQ_{AB}$ this switches to a positive, smaller bias (~1 ppb). Furthermore, the other, higher levels show little bias (~0.08 ppb). Thus comparing the TES and CMAQ profiles level-by-level indicates that the $CMAQ_{AB}$ scenario performs the best in simulating the TES retrievals, consistent with the conclusions based on the surface observations in Section 4.1."

*6) Aircraft observations: Possible artifacts? Include the uncertainties in the discussion of the results / conclusions.*

We have added Page 5, lines 25-30 to better explain artifacts and uncertainties from aircraft measurements using the CIMS instrument and added an additional reference (Nowak et al., 2007) and point to these uncertainties in the Discussion Section (Page 14, line 4). The new lines are as follows:

> "The CIMS instrument sampled air through a 0.55 m long heated teflon inlet with a fast flow. Measurement artifacts were accounted for by quantifying and subtracting the background signal originating from $NH_3$ desorption from instrument surfaces. The background signal was determined in flight by actuating a teflon valve at the inlet tip once every half hour to divert the sample air through a

> scrubber that removes $NH_3$ from the ambient air stream (Nowak et al, 2007). Additionally, standard addition calibrations from a $NH_3$ permeation tube were performed several times each flight to determine instrument sensitivity."

*7). Model: Some discussion on performance of the model for the vertical distribution of NH3 would be helpful.*

We have provided an additional flight curtain plot showing changes in vertically modeled $NH_x$ for the $CMAQ_B$ run (Figure 5c) as well as added discussion of these results aloft (Page 12, lines 6-11). Table 2 also includes statistics for the $CMAQ_{AB}$ runs as compared to flight measurements. In general we see an increase aloft in $NH_x$ from increased net land-atmosphere flux from the bidirectional $NH_3$ calculations.

> "Figure 5c is consistent with these results (and inconsistent with the hypothesis that vertical mixing is underestimated in the model) as the vertically distributed concentration of $NH_x$ significantly increases from the $CMAQ_{base}$ case to the $CMAQ_B$ case. The transport of $NH_3$ also tends to increase, this being a potential explanation for the plume entering the plot domain around 21:00 PDT in the bottom curtain plot. The total column concentration of $NH_3$ also increases, leading to a significant positive model bias for the $CMAQ_{AB}$ and $CMAQ_B$ scenarios (e.g. in the earlier part of the flight in Figure 5c and Table 2), suggesting a possible overestimation of total $NH_x$ emissions by the bi-directional $NH_3$ scheme during the afternoon and evening hours that the flights took place."

We have also included an additional figure (Figure 8, below) that follows a similar evaluation performed in Shephard et al. (2015) and is described in comment response # 5.

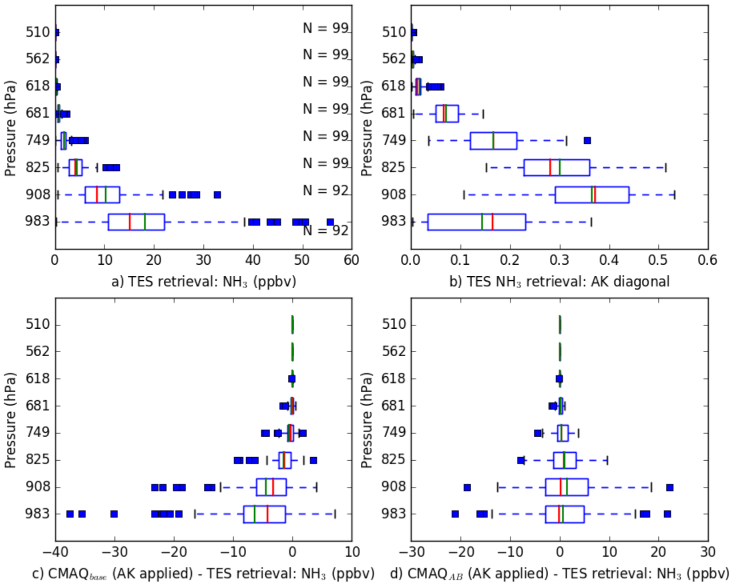

Figure 8. Boxplots of a) TES $NH_3$ retrieval by pressure level, b) TES $NH_3$ retrieval averaging kernel (AK) diagonal, c) difference between the TES $NH_3$ retrieval and $CMAQ_{base}$ modelled $NH_3$ interpolated to TES levels with an AK applied for the baseline model run and d) same as c) but for the $CMAQ_{AB}$ run. Box plots show the mean (green), median (red), interquartile range (IQR, blue box), whiskers at 1.5 IQR and outliers beyond that.

*8) Also include some words on the performance for species like HNO3 and sulfates as these are probably causes for any discrepancies in the diurnal cycle.*

We have included a ground measurement analysis plot for $HNO_3$ and $SO_4$ in the supplement (Figure S3), but we note that our method of primarily looking at $NH_x$ in our aircraft and surface evaluations removes potential errors due to incorrect gas-particle partitioning of $NH_3$, and that gas-phase $NH_3$ dominates the $NH_x$ concentration in this region. Thus we have not provided and evaluation of modeled $HNO_3$ and $SO_4$ in the main paper. The discussion added to the paper regarding these results is on Page 12, lines 10-16 and quoted below.

> "As noted above, the results for $NH_{3(g)}$ generally track the results for $NH_x$ already discussed. In contrast, the model usually under-predicts the small amount of $NH_{4(p)}$ observed (on average < 1 ppbv, Figure 2c) by

a factor of 2, with little variation between the model scenarios (Table 1). These model errors in $NH_{4(p)}$ reflect not only model errors in total $NH_x$, but also errors in the formation of $HNO_{3(g)}$ and $SO_{4(p)}$ (Figure S3). $HNO_{3(g)}$ is overestimated in all model simulations up to a factor of 4, with concentrations not changing between model cases. $SO_{4(p)}$ measured concentrations are minimal and don't appear to have any trend and also do not change with model cases. However, as our interest in this study is in constraining $NH_3$ emissions, not inorganic aerosol formation, we do not investigate these errors further here."

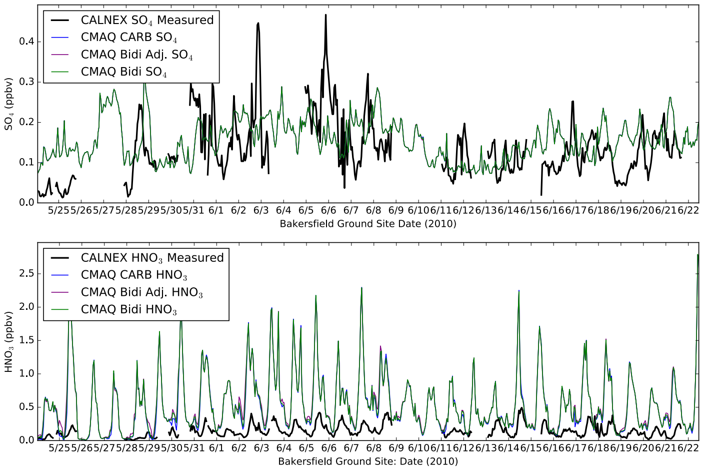

Figure S3. The CalNex ground measurements at the Bakersfield site (solid black) compared to the $CMAQ_{base}$ (solid blue), $CMAQ_{AB}$ (purple) and $CMAQ_B$ (green) simulations for a month of model runs. The top panel (a) shows $SO_{4(p)}$, b) shows $HNO_{3(g)}$

*9) 2.3. PBL: Figure 7 shows the performance of the WRF PBL when compared to the HSRL observations. The authors conclude that the deviations are not a probably cause for any faults in the diurnal cycle of NH3. I do not agree with this conclusion. From the plot one can conclude that for small PBL heights there are large deviations up to a factor 2 when compared to the modelled WRF PBL. You can convince me by showing a figure of the diurnal cycle of the PBL for both HSRL and WRF? And/or the normalized version of the cycle? By adding a diurnal cycle figure you also strengthen any comments and conclusions in the paper that the errors in the PBL have no effect.*

We have replaced the scatter plot with a time series of HSRL and WRF PBL (Figure 4 in the revised paper) in order to identify any diurnal patterns. The results from the scatter plot remain in the text for reference and in the Supplement Material (Figure S4). Although flight measurements only last a few hours and the diurnal cycle cannot be determined from these measurement comparisons, the plot does show that for small PBL heights the deviations are no greater than for higher heights and there do not appear to be any biases that could significantly contribute to the diurnal cycle of $NH_3$.

*10) 2.x Emissions: Can you add a table or a short paragraph on the emissions sources and their relative totals?*

We have added a table to the supplement (Table S2) that describes the fraction of CARB $NH_3$ emissions by source for the counties in the San Joaquin Valley and added a discussion on how this may impact the model results (Page 11, lines 19-22).

> "For Kern County, where Bakersfield, CA resides, pesticide/fertilizer applications dominate the $NH_3$ emissions inventory at 72%, followed by farming operations at 25%, and other sources for the remaining fraction. Table S2 in the Supplemental Material describes the fraction of $NH_3$ emissions for counties in the SJV."

*11) 3.3 Hysplit, I think this section can be removed as in the remainder of the paper only 3 sentences are dedicated to the results.*

We agree with the reviewer and have removed the HYSPLIT figure from the paper and added it to the supplemental material (Figure S2). However, we kept the discussion of the HYSPLIT model results as we feel addressing the direction from which emissions may have come is important in understanding the $NH_3$ cycle in the area.

*12) 4. Results: A bit of extra structure and discussion in the results will greatly improve the manuscript.*

We agree with the reviewer and have re-arranged sections so as to organize the paper around the three measurement platforms (Section 4.1 surface, Section 4.2 flight and Section 4.3 satellite) a new Discussion Section (Section 5) and an improved Conclusion Section (Section 6), as described in the introduction to the model evaluation section and earlier in this reviewer response. The response to comment 14 below describes the new Discussion Section in more detail.

*13) The authors have a wealth of data available but only scarcely use it. The flight data is only used for the basic version of the model, and not discussed in the latter parts of the manuscript, while the variation in the emissions will also affect the vertical distribution of the $NH_3$ concentrations.*

In addition to expanding our model sensitivity evaluations to a full month, we have also extensively added to the model comparisons to flight data. This includes a much more in-depth table (Table 2) which now includes flight data comparison to all model runs, as well as an added figure (Figure 5c) that demonstrates the changes in the vertical profile of $NH_x$ when the bi-directional ammonia scheme is applied. In general model concentrations increase in both the surface layer and aloft due to an increase in the net land-atmosphere flux, which can be interpreted as a combination of decreased deposition and increased emissions. However, this also increases the mean bias considerably (+7-10 ppbv) as seen in Table 2, and discussed on Page 12, lines 28-33 and Page 13, lines 1-3.

> "The $CMAQ_{base}$ run does not take this into consideration, but when the bidirectional flux exchange of $NH_3$ is calculated in $CMAQ_{AB}$ and $CMAQ_B$, $NH_3$ dry deposition should generally decrease, increasing the net land-atmosphere flux (Bash et al., 2013). Figure 5c is consistent with these results (and inconsistent with the hypothesis that vertical mixing is underestimated in the model) as the vertically distributed concentration of $NH_x$ significantly increases from the $CMAQ_{base}$ case to the $CMAQ_B$ case. The transport of $NH_3$ also tends to increase, this being a potential explanation for the plume entering the plot domain around 21:00 PDT in the bottom curtain plot. The total column concentration of $NH_3$ also increases, leading to a significant positive model bias for the $CMAQ_{AB}$ and $CMAQ_B$ scenarios (e.g. in the earlier part of the flight in Figure 5c and Table 2), suggesting a possible overestimation of total $NH_x$ emissions by the bi-directional $NH_3$ scheme during the afternoon and evening hours that the flights took place."

*14) The systematic discussion of possible causes for the discrepancies between the modelled and measured concentrations as given in 4.2 should be added for the other versions of the model. Each version should rule out one or more of the possible causes, which will add to the overall discussion of the state of the model (and not just this model, but the overall performance of most CTMs).*

As noted above, we have significantly expanded our discussion of the discrepancies between the modeled and measured concentrations for al three scenarios in Section 4, and have added a new Discussion Section (Section 5) that discusses the remaining errors in the $CMAQ_{AB}$ scenario and suggests avenues for further model improvement. We find that all three datasets suggest that the remaining errors in modelled $NH_x$ concentrations in $CMAQ_{AB}$ are due to the diurnal profile of the net land-atmosphere $NH_3$ flux in the $CMAQ_{AB}$ run peaking too late in the day or due to errors in the dynamic emissions response of the bi-directional $NH_3$ scheme to local temperature and wind speed conditions (Bash et al., 2013). For example, this could be due to errors in the dependence of soil conditions (e.g., soil temperature, pH, and water content) on meteorology and crop management practices as calculated within the bi-directional $NH_3$ scheme (Cooter et al., 2012). Additionally, aircraft results may also suggest errors in the vertical mixing of $NH_x$ during the afternoon and evening (e.g., the peak of the PBL height and the collapse). While we consider this effect as likely less important to the remaining errors in

$CMAQ_{AB}$ than the potential errors in the bi-directional $NH_3$ scheme, an overestimate of vertical mixing during the afternoon would overestimate the flux of $NH_x$ from the surface layer of the atmosphere to the upper levels, consistent with the aircraft overestimate. In addition, the soil-canopy-surface atmosphere system would respond to this overestimate of vertical mixing by increasing the net flux of $NH_x$ from the soil to the atmosphere in order to maintain equilibrium, resulting in a total overestimate of the emissions of $NH_x$ during the afternoon and evening.

*15) Adding a table with the airborne observations vs each of the modelled versions would help. Table 2. add some correlations and statistics similar to table 1.*

As described above, we have included more detailed tables (Table 1 - ground measurements, Table 2 - flight measurements and Table 3 - satellite comparison) that describe the statistics for all model scenarios.

*16) A figure or table in which you split the statistics per hour of the day will give some further insight on the performance of the model for each part of the day. Partially this is done already in figure 4, but some correlations / bias plot could be added for more information. In this figure/table one can then easily point out the improvements in the later model versions similar to figure 8.*

We have kept the flight measurement comparison for May 24, 2010 split up by time as well as Figure 3 which contains the average hourly ratio of $CMAQ_{base}$ modelled to measured $NH_3$ and $NH_x$ mixing ratios and the average $CMAQ_{base}$ modelled RVMR to TES RVMR ratio, a boxplot of average hourly $CMAQ_{base}$ modelled and measured $NH_x$ mixing ratios for the Bakersfield ground site, averaged over all measurement days during CalNex. We feel that the new Figure 9, similar to Figure 3 but for $CMAQ_{AB}$ results, demonstrates results that contain a model bias in the afternoon-evening hours, with slightly higher concentrations in the afternoon peaking around 19:00 (Figure 9b). We attribute these remaining errors to a few possible reasons discussed in comment # 14 and in more detail in the new Discussion Section 5.

*17) 5. Conclusion / Discussion: I am missing a final discussion on how one would improve the model in the future or what kind of measurements would be needed (does not have to be long). A few points for a start of the overall discussion and state of CMAQ/NH3 modelling (bit broad):*

*What kind of measurements would the authors perform to further understand the model and reasons for discrepancies between modelled and observed concentrations – Discuss point by point what this study improved, for now I can only see a small improvement to the bias. -- Final words: I recommend rewriting some parts of the manuscript following a few of the stated highlights to improve the overall quality of the paper. When rewritten this paper can be a great start for future model (improvement) studies.*

We thank the reviewer for their helpful comments regarding suggestions for a better organization of the paper and their technical comments. We feel that with our new organization of the Results, Discussion, and Conclusions section, described above, and the additional technical improvements made as suggested by the reviewer, the revised manuscript has been improved to better communicate both the model results and our recommendations about future steps towards future model improvements.

**Reviewer #2**

*1) General comments: This study presents a study combining surface, aircraft and satellite measurements of NH3 and NH4 concentrations in the San Joaquin Valley with a model study using CMAQ. The approach taken enables the authors to identify lacks in knowledge in both model description and emission inventories. While this is a worthwhile effort, the analysis and discussion could be improved by more explicitly including a discussion section in which the possible explanations of mismatch between model and observation are listed, as well as an outlook section with possible improvements to the model or emission data. If these points are improved upon (I give a few suggestions below), this paper could really contribute to improving NH3 modelling and to a better understanding of the sources of mismatch between model and measurements.*

We agree with the reviewer's comment that the paper could be improved by adding an explicit Discussion Section as well as a discussion of possible future model and inventory improvements. We have addressed this by, first, rearranging the model results section (Section 4) to organize the paper around the three measurement platforms (ground, flight and satellite measurements) rather than around the different model sensitivity studies. Section 4.1 in the new manuscript evaluates a full month of output from the three different model scenarios, $CMAQ_{base}$, $CMAQ_B$ (bidirectional ammonia) and $CMAQ_{AB}$ (bidirectional and adjusted emissions), with the surface measurements. We thoroughly discuss the evaluation of the diurnal distributions of $NH_x$, $NH_{3(g)}$ and $NH_{4(p)}$ in the three scenarios, since the surface measurements provide the best available information for identifying diurnal patterns. Section 4.2 discusses the aircraft measurement comparisons as well as the vertical profile of $NH_x$, since the aircraft measurements provide insight into the vertical dispersion of $NH_x$ as well as the overall magnitude of emissions in the afternoon and evening hours. Section 4.3 discusses the comparison of the three scenarios with the TES retrievals, including an added level-by-level comparison of the modeled and retrieved vertical profiles of $NH_3$. The new Discussion Section (Section 5) then describes the remaining errors in the final model version ($CMAQ_{AB}$) and suggests possible explanations for these errors and directions for future research. The revised Conclusions Section (Section 6) summarizes the results and discussion, and now includes a description of the overall model bias changes as well as suggestions for future work on $NH_3$ modeling in the SJV.

The new Discussion Section states that all three datasets suggest that the remaining errors in modelled $NH_x$ concentrations are due to the diurnal profile of the net land-atmosphere $NH_3$ flux in the $CMAQ_{AB}$ run peaking too late in the day, possibly due to errors in the dynamic emissions response of the bi-directional $NH_3$ scheme to local temperature and wind speed conditions (Bash et al., 2013). For example, this could be due to errors in the dependence of soil conditions (e.g., soil temperature, pH, and water content) on meteorology and crop management practices as calculated within the bi-directional $NH_3$ scheme (Cooter et al., 2012). Additionally, the aircraft results also suggest errors in the vertical mixing of $NH_x$ during the afternoon and evening (e.g., the peak of the PBL height and the collapse). While we consider this effect as likely less important to the remaining errors in $CMAQ_{AB}$ than the potential errors in the bi-directional $NH_3$ scheme, an overestimate of vertical mixing during the afternoon would overestimate the flux of $NH_x$ from the surface layer of the atmosphere to the upper levels, consistent with the aircraft overestimate. In addition, the soil-canopy-surface atmosphere system would respond to this overestimate of vertical mixing by increasing the net flux of $NH_x$ from the soil to the atmosphere in order to maintain equilibrium, resulting in a total overestimate of the emissions of $NH_x$ during the afternoon and evening.

We recommend that future modelling work includes updating the CARB $NH_3$ inventory to account for $NH_3$ from fertilizer, livestock, and other farming practices separately, as well as adding information on crop management practices specific to the SJV region to the EPIC-FESTC system. We also recommend top-down studies that focus not just on correcting the net $NH_x$ flux to the atmosphere but also on determining the diurnally-varying biases in the canopy compensation point that determines these net fluxes.

*2) Specific comments: For readers not familiar with the SJV geography and the location of the Bakersfield site, providing a map of the region could be valuable.*

We agree and have provided a new Figure 1 in the paper and below that shows the geography in California's SJV as it relates to $NH_3$ emissions.  In addition, this plot shows the location of the three measurement platforms used, in a map display. We have also provided a Table S2 (in the Supplement and below) that details the fraction of $NH_3$ emissions from different area sources in the SJV.

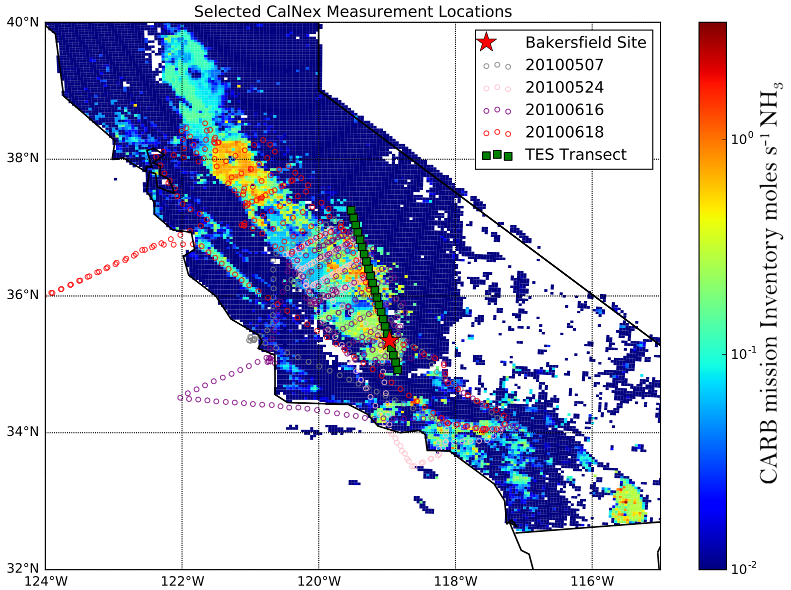

Figure 1. Distribution of $NH_3$ emissions across California (background) on May 12, 2010 at 19:00 UTC as well as P3 flight tracks (small circles), TES transect (green squares), and the Bakersfield site (red star)

Table S2. Contribution of sources to $NH_3$ emissions inventory in the San Joaquin Valley as reported in the CARB emissions inventory.

| County | Pesticide/ Fertilizer Fraction | Farming Operation Fraction | Other Area Sources |
|---|---|---|---|
| Kings County | 0.47 | 0.55 | 0.00 |
| Fresno County | 0.40 | 0.57 | 0.03 |
| Kern County | 0.72 | 0.25 | 0.03 |
| Merced County | 0.23 | 0.76 | 0.01 |
| Stanislaus County | 0.32 | 0.65 | 0.03 |
| Madera County | 0.33 | 0.64 | 0.03 |
| San Luis Obispo County | 0.25 | 0.51 | 0.24 |
| Tulare County | 0.11 | 0.86 | 0.02 |

*3) Title: Not everyone is familiar with CalNex. Adding 'campaign' (or otherwise clarifying the term) at the end of the title would make it clearer.*

We agree with the reviewer and have added 'campaign' to the title that now reads "Modeling the Diurnal Variability of Agricultural Ammonia in Bakersfield, California during the CalNex Campaign".

*4) Introduction: While the introduction presents a thorough overview of previous work, it is rather elaborate. Condensing this by focusing on the most important points would increase readability. This is later also true for the description of the TES data and the CMAQ model.*

We agree with the reviewer's comment and have made an effort throughout the paper to condense discussion, and also feel with the improvements made based on both reviewer's comments that the overall paper readability has been improved. For example, we have removed paragraphs in the Introduction Section (Page 3, lines 25-27 in the original manuscript) and Section 3.2 (Page 8, lines 20-25 in the original manuscript) that we felt were not necessary for background understanding of the manuscript.

*5) Please specify at some point in which period the CalNex campaign was active.*

The CalNex campaign ran in May and June of 2010 as stated in the paper on Page 4, line 15.

*6) Data: Please give coordinates and elevation of the Bakersfield site.*

We have provided coordinates and elevation of the Bakersfield surface site, Page 6, line 5 – "Bakersfield, California is located on the southern part of the SJV (35.35°N, 118.97°W, 20 m asl)"

*7) Models: In the text on the CMAQ model results of sensitivity studies are already provided. Consider moving this to the results section. You could also consider dedicating a paragraph to the description of the emission database (which are the most important ammonia sources, etc.) as this is so important in your uncertainty analysis later.*

We have made sure no results are described in sections previous to Section 4 and have added a discussion on the $NH_3$ emissions database (Page 11, lines 19-22) to the paper:

> "For Kern County, where Bakersfield, CA resides, pesticide/fertilizer applications dominate the $NH_3$ emissions inventory at 72%, followed by farming operations at 25%, and other sources for the remaining fraction. Table S2 in the Supplemental Material describes the fraction of $NH_3$ emissions for counties in the SJV."

We have also improved Figure 1 to demonstrate the spatial distribution of $NH_3$ sources in the SJV and have included a table that describes the break down of area ammonia sources in the Supplement (Table S2), as described in comment 2.

*8) Page 8, line 32: ' . . . soil emissions potential and NH4': sentence is incomplete.*
We have restructured and completed this description sentence now on Page 9, lines 19-21:

> "Finally, we also ran CMAQv5.0.2 using the bi-directional $NH_3$ flux scheme as developed by Bash et al. (2013) that uses fertilizer application data, crop type, soil type, and meteorology from MCIP output to calculate soil emissions potential and $NH_4$ to simultaneously calculate $NH_3$ deposition and emission fluxes for the CMAQ US domain."

*9) Results:*
*Section 4.1: You claim that the relative changes in NH3 concentration along the transect are captured well by the model, but to me this seems not to be the case: the highest concentrations are underestimated much more strongly, also in a relative sense, than the lower concentrations outside the direct source region. Also, based on figure 3 you conclude that CMAQ with the CARB inventory captures the spatial variability near Bakersfield well, but given the correlation coefficient of 0.22 for the overpasses closest to Bakersfield I'm not sure this statement holds. The purpose of highlighting these points is not clear as it is later not at all discussed. If I understand the plot and caption correctly, each point represents one overpass in one grid cell, i.e., this plot shows both temporal and geographical variability. Is this correct? If yes, could you comment on which part of the scatter is caused by temporal and which by geographical variability?*

We have clarified the discussion of model results compared to the TES overpass in Section 4.3 and improved the wording on the relative correlation comparisons. Figure 2 from the original paper (now Figure 6 in the revised paper) demonstrates that the $CMAQ_{RVMR}$ is consistent with the location of higher concentrations of $NH_3$ as seen in the $TES_{RVMR}$. We have also clarified our comments on the temporal/geographical variability – in general there is no actual temporal variability in the TES-CMAQ plots, since CMAQ output is hourly and only the hour corresponding to the TES overpass is shown.Thus there is only geographical variability. The description now reads (added, Page 13, lines 5-10):

> “Figure 6a shows the RVMR retrieved from the TES spectra ($TES_{RVMR}$) for one overpass (during one hour of model output) on 12 May 2010; the other overpasses during the campaign are similar. Figure 6b shows the equivalent $CMAQ_{base}$ modelled $NH_3$ RVMR ($CMAQ_{RVMR}$) (see Equation 1 and 2 in Section 2.2), and Figure 6c shows the difference between the two. This figure demonstrates that the $CMAQ_{base}$ case can identify the locations of different sources of $NH_3$ and the resulting geographical relative changes in $NH_3$ along the transect, but that the $NH_3$ RVMRs are underestimated, particularly at higher $NH_3$ RVMRs (Table 3 and Table S2).

The graph below shows the average TES RVMR (ppb) for each overpass day during the CalNex campaign. It can be seen that no additional temporal trends could be discerned (i.e. on a month-to-month basis) and thus this potential temporal variability was not discussed in the paper.

| Date | Average TES RVMR (ppb) | Std Dev. TES RVMR (ppb) |
|---|---|---|
| 2010/05/12 | 8.59 | 7.99 |
| 2010/05/14 | 6.54 | 6.00 |
| 2010/05/28 | 4.55 | 2.99 |
| 2010/05/30 | 6.33 | 6.19 |
| 2010/06/13 | 8.26 | 5.69 |
| 2010/16/15 | 8.47 | 5.53 |

*10) Section 4.2: From figure 4 I don’t see an underestimation of a factor 2.5 during the daytime, rather 1.5-2.*

We thank the reviewer and realize how this could be interpreted as 1.5 to 2 and have corrected this on Page 10, lines 13-19 to now say:

> “The model bias shows a clear diurnal cycle, with $CMAQ_{base}$ significantly overestimating surface $NH_x$ concentrations at night by up to a factor of 4.5 and generally underestimating $NH_x$ during the daytime at 0.6 between 13:00 and 14:00 local time, consistent with the average $TES_{RVMR}$ observations near Bakersfield at about 13:30 local solar time plotted as the green dot in Figure 3a and further discussed in Section 4.3. These results suggest that the constant daily emissions for agricultural $NH_3$ emissions in the CARB inventory (blue line, Figure S1 in the Supplemental Material) may be misrepresenting the diurnal emission patterns suggested by the measurements. This is consistent with previous work done in North Carolina; Wu et al. (2008) found that $NH_3$ emissions from livestock feed lots show a strong diurnal cycle, peaking at mid-day.

*11) Line 26-27 (page 9) would be better supported by adding a time series of the measurement-model comparison to show the seasonal patterns.*

We agree with the reviewer and have added a new Figure 2, that now includes a full month comparing model results to ground measurements for $NH_x$, $NH_{3(g)}$, $NH_{4(p)}$, temperature, and wind speed. The temporal scope of these measurements, however, is only May and June so longer seasonal patterns cannot be evaluated with this dataset.

*12) Lines 3-6 (Page 10) seem redundant.*

We agree with the reviewer and have removed this section.

*13) Lines 13 and onwards (page 10): please mention that you now compare concentrations at 400+ meters above the surface; otherwise the step from the ground-based observations to air craft might be confusing.*

We have re-worded the sentence (now on Page 12, line 10) and elsewhere to include the fact that these measurements are taken at higher altitudes, as shown in Figure 5.

> "The aircraft observations in the SJV indicate a large underestimate (range of factors about 1 to 5) in $CMAQ_{base}$ modelled $NH_x$ concentrations at higher altitudes as shown in Table 2 (all flights in SJV) and Figure 5 (two flights)."

*14) Page 10, line 28 – page 11, line 7: This section can be shortened significantly; consider if results that are not worth showing are worth talking about.*

With the re-arranging of the model results section, and the addition of the new Discussion Section we feel that all results presented now are worth discussion. We have also excluded the plot of a brief HYSPLIT analysis that is only worth mentioning to rule out significant diurnal changes in source region that potentially could have contributed to biases in modeled concentrations, but do not appear to.

*15) Section 4.3: What does 'consistent with measured temperature patterns' mean? I assume it suggests that temperature is the driving variable for the emission variability during the day, could you state that more clearly?*

We realize the initial reference to temperature patterns was confusing. We now include model and measured temperature at the Bakersfield site, Figure 2d and discuss how temperature variability could influence modeled concentrations (Page 14, lines 27-33, and Page 15, lines 1-4):

> "Thus the remaining errors are less likely related to errors in atmospheric meteorological conditions, and are more likely due to errors in the dependence of soil conditions (e.g., soil temperature, pH, and water content) on meteorology and crop management practices as calculated within the bi-directional $NH_3$ scheme (Cooter et al., 2012). The scheme calculation assumes two soil layers (0.01 m and 0.05 m) that independently exchange $NH_x$ with the canopy, which then exchanges $NH_x$ with the surface layer of the atmosphere (Bash et al., 2013). If the calculation of the response of soil properties in these layers to surface meteorology and crop management practices is incorrect (e.g., the soil layers do not heat up or cool down quickly enough with the change in surface temperature), that would affect the amount of $NH_x$ available from the soil as well as the rate at which the soil $NH_4^+$ is converted to $NO_3^-$ through nitrification (Bash et al., 2013). This would result in errors in the flux of $NH_x$ from the soil to the canopy, thus altering the canopy compensation point and the net atmospheric flux."

*16) Why did you only adjust the hourly emission profile for NH3, was there no day-to-day variability (e.g. related to temperature) to take into account? With the approach taken, you assume that concentrations in a certain hour are dominated by emissions in that same hour; could you comment on this assumption?*

We focused on the diurnal errors, as these errors can complicate the interpretation of data sets, such as the aircraft and TES observations, that do not cover the entire diurnal cycle. While temperature certainly varies day-to-day, and this should affect $NH_3$ emissions, we are less confident that there is sufficient variability in temperature during our one-month evaluation period to constrain this variability. Other varying factors, such as source location, planetary boundary layer height, and gas-to particle partitioning, are discussed and do not show significant enough biases to explain modeled $NH_3$ concentration bias.

The model appears to capture the day-to-day meteorological variability well, as seen in Figure 2d, which shows the modelled and measured surface temperature and wind speed. We do feel, however, that errors in the dependence of soil conditions (e.g., soil temperature, pH, and water content) on meteorology and crop management practices as calculated within CMAQ may be contributing to the modelled $NH_3$ bias. Additionally, the aircraft results also suggest errors in the vertical mixing of $NH_x$ during the afternoon and evening and while we consider this effect as contributing less to the remaining errors in the model, an overestimate of vertical mixing during the afternoon would overestimate the flux of $NH_x$ from the surface layer of the atmosphere to the upper levels. Thus, we recommend that future work to improve the simulation of atmospheric $NH_x$ concentrations in the SJV focus on bottom-up and top-down approaches that will better estimate the diurnal changes in the canopy compensation point that determines the net flux from the land to the atmosphere in the bi-directional $NH_3$ scheme (Bash et al., 2013). This is discussed in more detail in the new Discussion Section 5.

*17) Why did you decide to test the new diurnal profile for 7 days only? A comparison to the aircraft data would be valuable here as well, to see to what extent the changed diurnal profile impacts modelled concentrations and model performance at higher altitudes.*

As noted previously, we have extended the time series of all model runs to cover an entire month (May 22 – June 22) which covers the complete Bakersfield super site record for $NH_x$. Figure 2 compares our three model scenarios to the ground measurements for $NH_x$, $NH_3$, and $NH_4$ for this entire period, and the statistics for this period are shown in the new Table 1. In addition, we have added an additional plot of aircraft data compared to the $CMAQ_B$ run (Figure 5c), which shows the impact that the calculation of bi-directional exchange of ammonia has on the model performance at higher altitudes. The statistics for these flight comparisons are also shown in Table 2.

*18) Section 5: This section would be stronger if it contained more than a summary of the most important points of the paper, but also a discussion on future steps / important work to be done to improve the modelling of ammonia and the representation of emissions. For example, a discussion on the relative importance of the misrepresentation of emission diurnal cycles vs. misrepresentation of the vertical mixing (which should we work on first?) would be valuable.*

We thank the reviewer for this valuable recommendation and feel that the new Discussion Section, described in comment # 16 above, emphasizes the relative importance of several aspects that could improve the diurnal modeling of ammonia.

*19) Technical comments:*
*Page 2, line 6: photoxidize should be photo-oxidize*

We have corrected this typo.

*20) Page 3, line 11: CONUS might not be a known acronym for non-US readers; please explain.*

We have removed CONUS and replaced with ‘continental US’

*21) Page 3, line 25: Write out TES as it is the first mention in the main body of the article. In general: check for unexplained abbreviations.*

We have added this and checked the paper for other abbreviations not defined.

*22) Page 7, lines 11 and 12: HSRL is mentioned as acronym but only written fully at the second instance.*

We have corrected this by adding the acronym description the first time it is mentioned, Page 4, line 27.

*23) Page 8, line 14: SoCAB is not explained.*

We thank the reviewer for pointing out this referenced term in the paper. This sentence and the one following it describe emissions in the southern and LA areas, unrelated to the emissions in the SJV, thus we removed these 2 sentences.

*24) Page 9, line 13: scatterplot should be scatter plot*

We have corrected this typo

*25) Page 11, line 23: remove 'mostly' as the CARB NH3 emissions are completely constant.*

We have removed 'mostly' from the description of the daily emissions pattern.

# Modeling the Diurnal Variability of Agricultural Ammonia in Bakersfield, California during the CalNex Campaign

C. R. Lonsdale[1], J. D. Hegarty[1], K. E. Cady-Pereira[1], M. J. Alvarado[1], D. K. Henze[2], M. D. Turner[2], S. L. Capps[2], J. B. Nowak[3,4,*], J. A. Neuman[4], A. M. Middlebrook[4], R. Bahreini[4], J. G. Murphy[5], M. Z. Markovic[5**], T. C. VandenBoer[5***], L. M. Russell[6], A. J. Scarino[7]

[1]Atmospheric and Environmental Research, Lexington, MA, USA
[2]Department of Mechanical Engineering, University of Colorado, Boulder, CO, USA
[3]Cooperative Institute for Research in Environmental Sciences, University of Colorado Boulder, CO, USA
[4]Chemical Sciences Division, Earth System Research Lab, NOAA, Boulder, CO, USA
[5]Department of Chemistry, University of Toronto, Toronto, ON Canada
[6]Scripps Institution of Oceanography, University of California, San Diego, CA, USA
[7]Science Systems and Applications Inc., Hampton, VA, USA
*Now at Aerodyne Research, Inc. Billerica, MA, USA
**Now at Picarro, Inc., Santa Clara, CA, USA
*** Now at Department of Earth Sciences, Memorial University of Newfoundland, NL Canada

*Correspondence to*: C. R. Lonsdale (clonsdal@aer.com)

Chantelle Lonsdale 6/21/2016 10:03 AM
**Deleted:** Air Quality Research Division, Environment

Chantelle Lonsdale 6/21/2016 10:03 AM
**Deleted:** , Toronto, ON, CA

**Abstract.** $NH_3$ retrievals from the NASA Tropospheric Emission Spectrometer (TES), as well as surface and aircraft observations of $NH_{3(g)}$ and submicron $NH_{4(p)}$, are used to evaluate modelled concentrations of $NH_{3(g)}$ and $NH_{4(p)}$ from the Community Multiscale Air Quality (CMAQ) model in the San Joaquin Valley (SJV) during the California Research at the Nexus of Air Quality and Climate Change (CalNex) campaign. We find that simulations of $NH_3$ driven with the California Air Resources Board (CARB) emission inventory are qualitatively and spatially consistent with TES satellite observations, with a correlation coefficient ($r^2$) of 0.64. However, the surface observations at Bakersfield indicate a diurnal cycle in the model bias, with CMAQ overestimating surface $NH_3$ at night and underestimating it during the day. The surface, satellite, and aircraft observations all suggest that daytime $NH_3$ emissions in the CARB inventory are underestimated by at least a factor of two, while the night-time overestimate of $NH_{3(g)}$ is likely due to a combination of overestimated $NH_3$ emissions and underestimated deposition.

Running CMAQ v5.0.2 with the bi-directional $NH_3$ scheme reduces $NH_3$ concentrations at night and increases them during the day. This reduces the model bias when compared to the surface and satellite observations, but the increased concentrations aloft significantly increase the bias relative to the aircraft observations. We attempt to further improve the model by using the surface observations at Bakersfield to derive an empirical diurnal cycle of $NH_3$ emissions in the SJV, in which night-time and midday emissions differ by about a factor of 4.5. Running CMAQv5.0.2 with a bi-directional $NH_3$ scheme as well as this emissions diurnal profile further reduces model bias relative to the surface observations. Comparison of these simulations with the vertical profile retrieved by TES shows little bias except for the lowest retrieved level, but the

Chantelle Lonsdale 6/23/2016 7:09 AM
**Deleted:** , and insufficient vertical mixing in the Weather Research and Forecasting model (WRF) meteorological fields used to drive CMAQ.

Chantelle Lonsdale 6/23/2016 7:10 AM
**Deleted:** this diurnal profile ssimulation ) in The remaining model errors suggest that the bi-directional $NH_3$ scheme in CMAQ v5.0.2 errors in needs further improvements to shift the peak $NH_3$ land-atmosphere flux to earlier in the day. We recommend that future work include: ,;including revised in the bi-directional $NH_3$ scheme; and edland-atmosphere $NH_3$

model bias relative to flight data aloft increases slightly. Our results indicate that both diurnally-varying emissions and a bi-directional $NH_3$ scheme should be applied when modelling $NH_{3(g)}$ and $NH_{4(p)}$ in this region. The remaining model errors suggest that the bi-directional $NH_3$ scheme in CMAQ v5.0.2 needs further improvements to shift the peak $NH_3$ land-atmosphere flux to earlier in the day. We recommend that future work include: updates to the current CARB $NH_3$ inventory to account for $NH_3$ from fertilizer, livestock, and other farming practices separately; adding revised information on crop management practices specific to the SJV region to the bi-directional $NH_3$ scheme; and top-down studies focused on determining the diurnally-varying biases in the canopy compensation point that determines the net land-atmosphere $NH_3$ fluxes.

## 1 Introduction

The emissions of ammonia ($NH_3$) to the atmosphere are highly uncertain (e.g., Pinder et al., 2006; Beusen et al., 2008; Galloway et al., 2008; Henze et al., 2009; Schlesinger, 2009). Nitrogen dioxide ($NO_x = NO + NO_2$) and sulfur dioxide ($SO_2$) photo-oxidize in the atmosphere to form nitric acid ($HNO_3$) and sulfuric acid ($H_2SO_4$), respectively, which react with atmospheric gas-phase ammonia ($NH_{3(g)}$) to form ammonium sulfate ($(NH_4)_2SO_4$) and ammonium nitrate ($NH_4NO_3$) aerosol. Uncertainty in $NH_3$ emissions therefore leads to significant uncertainties in the concentrations of secondary inorganic aerosols. Ammonium sulfate and nitrate aerosols contribute to fine particulate matter concentrations ($PM_{2.5}$), and thus to decreased visibility, altered climate, and acidification and eutrophication in sensitive ecosystems (e.g., Paulot et al., 2014; RoTAP. 2012; Bricker et al., 2007; Martin et al., 2004).

Chantelle Lonsdale 6/21/2016 10:03 AM
**Deleted:** photoxidize

$PM_{2.5}$ also causes adverse health effects (WHO, 2016; Pope et al., 2004). In particular, some regions in the San Joaquin Valley (SJV) in California have been designated as non-attainment areas for $PM_{2.5}$, with $NH_3$ emissions contributing to more than half of the inorganic $PM_{2.5}$ in the state (Schiferl et al., 2014), depending on ambient conditions and concentrations (Lonsdale et al., 2012). During the NOAA California Research at the Nexus of Air Quality and Climate Change (CalNex) campaign in May and June of 2010, however, concentrations of $PM_{2.5}$ rarely exceeded the National Ambient Air Quality Standard (NAAQS) in the SJV, as $PM_{2.5}$ exceedances here generally happen in the winter. While emissions of $NO_x$ and $SO_2$ are relatively well constrained, are regulated by the United States Environmental Protection Agency (US EPA), and are predicted to continually decrease due to air quality regulations and emission reducing technologies (US EPA, 2010), $NH_3$ emissions are not currently regulated and are predicted to stay constant or increase over the next several decades in the US due to an increasing population and associated increases in farming and agricultural activities (Moss et al., 2010). Climate change is also predicted to increase $NH_3$ emissions (+0-40 % in north-central Europe) with larger countries having the largest uncertainty in emissions variations (Skjøth et al., 2013).

Chantelle Lonsdale 6/21/2016 10:03 AM
**Deleted:** 2013

Anthropogenic $NH_3$ sources in the SJV are dominated by agricultural activities, with livestock waste estimated to contribute about 74 % of total anthropogenic $NH_3$ to the atmosphere and chemical fertilizer use another 16 % (Simon et al., 2008). Agricultural emissions of $NH_3$ can be highly variable due to factors such as the differences in fertilizer application, the diet provided to livestock, and waste management and storage practices of farmers (Hristov et al., 2011; Sawycky et al., 2014). In addition, while $NH_{3(g)}$ can be quickly deposited to the surface causing soil acidification, water eutrophication, and an imbalance of ecosystems when in excess (e.g., Carfrae et al., 2004), the air-surface exchange of $NH_3$ is bi-directional, with the direction of the $NH_3$ flux between the land and the atmosphere varying with temperature, relative humidity, vegetation and soil type, maintenance (e.g., cutting and tilling practices), and fertilizer applications (Nemitz et al., 2001; Zhang et al., 2010; Ellis et al., 2011; Bash et al., 2013; Sawycky et al., 2014). This complexity in the emission and deposition of $NH_3$, along with the rapid reactions of $NH_3$ with $HNO_3$ and $H_2SO_4$ and the consequently short (~1 day) atmospheric lifetime of $NH_3$, leads to large temporal and spatial variability of this gas, as seen in in situ measurements (e.g., Langford et al., 1992; Carmichael et al., 2003; Nowak et al., 2010; Walker et al., 2013) and in satellite retrievals (e.g., Clarisse et al., 2013; Pinder et al., 2011; Shephard et al., 2011; Heald et al., 2012; Sun et al., 2015; Shephard and Cady-Pereira, 2015; Shephard et al., 2015).

Recent studies have recognized a diurnal pattern of $NH_3$ emissions from livestock attributed to potential differences in farm management practices, livestock housing outflow patterns, and variations in soil moisture, temperature, and wind speed (Hensen et al., 2009; Zhu et al., 2015a; Zhu et al., 2015b). To account for this, a diurnal variability scheme was implemented into global simulations using the global 3-dimensional chemical transport model, GEOS-Chem, and was shown to decrease $NH_3$ concentrations globally (Zhu et al., 2015a). That study also calculated the bi-directional exchange of $NH_3$, which decreased $NH_3$ concentrations in the US in the months of October through April and increased it in the month of July (Zhu et al., 2015a). Bash et al. (2013) also explored the sensitivity of modelled $NH_3$ concentrations to a bi-directional $NH_3$ scheme that used meteorological factors, including temperature, wind speed, agricultural crop flux values, and a nitrogen soil geochemistry parameterization in the CMAQ model. They found that over the continental US their model run with the bi-directional $NH_3$ scheme decreased the total dry deposition of $NH_3$ by 45 %, thus increasing atmospheric $NH_3$ concentrations and $NH_x$ wet deposition by 10 % and 14 %, respectively. Wichink Kruit et al. (2012) use the DEPosition of Acidifying Compounds (DEPAC) surface-atmospheric exchange module in a CTM and saw an increase in atmospheric $NH_3$ almost everywhere in their model domain, including decreased $NH_3$ deposition with a remaining underestimation in agricultural areas.

Previous studies have also shown that errors in $NH_3$ emissions are a common contributing factor to modelled $PM_{2.5}$ and $NH_3$ bias (e.g., Schiferl et al., 2014). Skjøth et al., (2011) discuss their method for calculating dynamic $NH_3$ emissions that includes distributions of agricultural $NH_3$ in Europe. Their method is designed for use in chemical transport models and their results show considerable improvements made in the agricultural $NH_3$ sector, particularly in areas with detailed records of agricultural practices. Inverse modelling studies have been used to reduce the uncertainty in $NH_3$ emissions as well, generally by assimilating surface observations of the wet deposition of ammonium ($NH_4^+$) in precipitation. Gilliland et al. (2003) used the CMAQ model to determine that the 1990 version of the US EPA National Emissions Inventory (NEI) overestimated total emissions of $NH_3$ by 20 %. Gilliland et al. (2006) performed a similar study for the 2001 NEI and found that total emissions of $NH_3$ were represented well, but needed to be increased in summer and reduced in winter. Henze et al.

Chantelle Lonsdale 6/22/2016 12:31 PM
**Deleted:** ,

Chantelle Lonsdale 6/22/2016 12:31 PM
**Deleted:** which is based on emission estimates and model inputs from State, Local and Tribal agencies (US EPA, 2015),

Chantelle Lonsdale 6/22/2016 12:31 PM
**Deleted:** this updated inventory represented the

Chantelle Lonsdale 6/22/2016 12:31 PM
**Deleted:** that $NH_3$ emissions

(2009) used the adjoint of the global chemical transport model GEOS-Chem to assimilate the Inter Agency Monitoring of Protected Visual Environments (IMPROVE) observations and found that total US $NH_3$ emissions for 1998 were overestimated.

Chantelle Lonsdale 6/22/2016 12:32 PM
**Deleted:** that the high nitrate concentrations in the model implied

More recently, satellite observations of $NH_3$ have been incorporated into inverse studies. By assimilating satellite retrievals of $NH_3$ concentrations from the Tropospheric Emission Spectrometer (TES) (Beer et al., 2008; Shephard et al., 2011) aboard the NASA Aura satellite, it has been found that $NH_3$ emission sources in GEOS-Chem are broadly underestimated (Zhu et al., 2013). Heald et al. (2012) and Walker et al. (2012) used IMPROVE data and satellite retrievals of $NH_3$ from the Infrared Atmospheric Sounding Instrument (IASI, Van Damme et al., 2014) to show that $NH_3$ emissions are likely underestimated in GEOS-Chem for California, leading to a local underestimate of $NH_{4(p)}$. Other infrared nadir sounders have been used to provide satellite observations of $NH_3$. For example, Shephard and Cady-Pereira (2015) demonstrated the ability of the Crosstrack Infrared Sounder (CrIS) aboard the joint NOAA-NASA Suomi National Polar-orbiting satellite to measure daily, spatially distributed tropospheric $NH_3$ in California, and in preliminary results found it correlated well with Deriving Information on Surface Conditions from Column and Vertically Resolved Observations Relevant to Air Quality (DISCOVER-AQ) measurements in the SJV in January 2013.

Chantelle Lonsdale 6/22/2016 1:57 PM
**Deleted:** the Inter Agency Monitoring of Protected Visual Environments (

Investigating the formation, transport, and fate of $NH_{3(g)}$ and $NH_{4(p)}$ in California was one of the major goals of the CalNex field campaign, which provided measurements from flights and surface sites (Ryerson et al., 2012). Nowak et al. (2012) used this data to demonstrate the importance of ammonium nitrate formation downwind of the Los Angeles urban core and dairy facilities further east. They found that $NH_3$ emissions from these dairy farms were underestimated by a factor of 3 or more, thus indicating the need for better representation in this emission sector. Kelly et al. (2014) in general saw well-correlated comparisons of CMAQ model estimates to measurements from the EPA's Chemical Speciation Network. Their model tended to under-predict $NH_x$ ($NH_x = NH_{3(g)} + NH_{4(p)}$) during the day at the Bakersfield, CA site and significantly over-predict $NH_{3(g)}$ at night. They suggest that this model bias may be due to emissions from livestock and dairy farms being too low and lacking in variability in this region or to errors in crustal cation predictions and the missing effects of organic acids and amines on inorganic aerosol thermodynamics (Kelly et al., 2014).

Chantelle Lonsdale 6/24/2016 10:04 AM
**Deleted:** performed in May and June 2010

Model estimates of the planetary boundary layer (PBL) height are essential in correctly quantifying changes in atmospheric pollutant concentrations, especially for short-lived pollutants like $NH_3$. Such estimates are difficult at fine spatial and temporal scales, especially in the complex terrain of the SJV. Scarino et al. (2014) studied the PBL and mixed layer heights during CalNex using WRF and high spectral resolution lidar (HSRL) data taken during the campaign. They found that, in general, there is good agreement between the WRF modelled output and measured values; however, in the California Central Valley there is a WRF mixed-layer height over-prediction and an inability to represent the diurnal growth of the mixed layer in the early part of the day. Additionally they suggest that future improvements will require a focus on mixing layer characteristics, soil moisture, and temperature. Baker et al. (2013) explored how well the WRF model configuration used to drive the CMAQ simulations of Kelly et al. (2014) simulates PBL height during CalNex, using two versions of WRF. The study shows that both WRF versions simulate the PBL and mixing layers well within the SJV, as well as other large scale

Chantelle Lonsdale 6/22/2016 9:39 AM
**Deleted:** and

flow patterns, but under-predict local wind speed and temperature. A strong aerosol gradient is used to identify the top of the PBL in HSRL measurements, which may also be present in a night-time residual layer. Baker et al. (2013) take this into account by identifying the surface-attached mixed layer, which they assume as the lowest significant gradient in such a circumstance.

In this study, we use the CalNex observations of $NH_{3(g)}$ and $NH_{4(p)}$ and the CMAQ model to evaluate the estimates of $NH_3$ emissions in the SJV contained in the California Air Resources Board (CARB) inventory (Figure 1). While previous $NH_3$ model evaluation efforts using CalNex data have focused on the NEI inventory (Kelly et al., 2014; Heald et al., 2012; Walker et al., 2012), the CARB inventory is used in the development of California's State Implementation Plans (SIPs) under the Clean Air Act, and so ensuring the accuracy of this emission inventory is important to the design of air quality policy for the SJV and California in general. In addition, previous studies have not taken advantage of the high-resolution observations of $NH_{3(g)}$ made by the TES satellite instrument over Bakersfield during the CalNex campaign. Here we evaluate the consistency of the satellite, aircraft, and surface observations of $NH_{3(g)}$ and $NH_{4(p)}$ during the CalNex campaign and then use these observations, along with lidar retrievals of PBL height, to investigate the biases in the magnitude and diurnal cycle of emissions of $NH_{3(g)}$ and from the CARB inventory in the SJV. We also explore the sensitivity of modelled $NH_3$ concentrations to bi-directional $NH_3$ exchange using the bi-directional $NH_3$ flux scheme in CMAQv5.0.2.

Section 2 briefly describes the data sources used in this study, while Section 3 describes the CARB emission inventory and the configurations used for the WRF, the Hybrid Single-Particle Lagrangian Integrated Trajectory (HYSPLIT), and CMAQ model runs. The performance of the CARB inventory used in our CMAQ simulations, along with model sensitivity studies, is presented in Section 4. Section 5 discusses the remaining errors in our final model configuration in detail and makes suggestions for further model improvements, while our conclusions are discussed in Section 6.

Chantelle Lonsdale 6/23/2016 7:10 AM
**Deleted:** the remaining errors in our final model configuration in detail makes suggestions for further whileour cdiscussed our suggested improvements to the CARB $NH_3$ inventory and summarizes our conclusions.

## 2 Data

### 2.1 NOAA WP-3 aircraft

Chantelle Lonsdale 6/21/2016 10:03 AM
**Deleted:** **CalNex campaign**

The NOAA WP-3 aircraft completed 18 research flights during the CalNex campaign, which included measurements of $NH_{3(g)}$ and $NH_{4(p)}$. $NH_{3(g)}$ was measured at 1 s (~100 m) intervals using chemical ionization mass spectrometry (CIMS) with an uncertainty of +/- 30 % as described in detail in Nowak et al. (2007). The CIMS instrument sampled air through a 0.55 m long heated teflon inlet with a fast flow. Measurement artifacts were accounted for by quantifying and subtracting the background signal originating from $NH_3$ desorption from instrument surfaces. The background signal was determined in flight by actuating a teflon valve at the inlet tip once every half hour to divert the sample air through a scrubber that removes $NH_3$ from the ambient air stream (Nowak et al, 2007). Additionally, standard addition calibrations from a $NH_3$ permeation tube were performed several times each flight to determine instrument sensitivity. Submicron $NH_{4(p)}$ was measured at 10 s (~ 1 km) intervals with an uncertainty of ~ 30 % using a compact time-of-flight aerosol mass spectrometer from Aerodyne (c-TOF AMS, Bahreini et al., 2009). In this study we focused on the flights of 24 of May and 16 and 18 of June when the WP-3

Chantelle Lonsdale 6/21/2016 10:03 AM
**Deleted:** (2010).

Chantelle Lonsdale 6/21/2016 10:03 AM
**Deleted:** 7 and

was sampling air in the SJV (Figure 1). The quality-controlled flight data were reported at a merged time resolution of 1 s, which we averaged to 1 minute values (the approximate time it takes the WP-3 to cross a 4 km CMAQ grid box) and then matched the sample times and locations to the corresponding time and location of the CMAQ hourly concentration output.

### 2.2 Bakersfield surface observations

Bakersfield, California is located on the southern part of the SJV (35.35°N, 118.97°W, 20 m asl) and there is a general north-to-south orographic air-flow in this region, with a tendency for emissions to get trapped in the valley due to the nearby mountains (Baker et al., 2013). At the Bakersfield ground site the Ambient Ion Monitor Ion Chromatograph (AIM-IC, Ellis et al., 2010, Markovic et al., 2012) was used to measure $NH_{3(g)}$ on an hourly basis, with an uncertainty of +/- 20 % and a detection limit of 41 ppt. The sampling inlet for the AIM-IC consists of an enclosure mounted at 4.5 m above ground, including a virtual impactor, parallel plate denuder, and particle supersaturation chamber, connected to the ion chromatography systems via several 20 m perfluoroalkyl sampling lines carrying the dissolved analytes (Markovic et al., 2014). This design reduces artifacts by minimizing the inlet surface area prior to scrubbing the $NH_3$ from the gas phase in the denuder, and by separating the gas and particle phase constituents while the sample flow is still at ambient temperature and relative humidity (Markovic et al., 2012). In addition, size-resolved, sub-micron non-refractory $NH_{4(p)}$ measurements were taken at 5 minute intervals using an Aerodyne Aerosol Mass Spectrometer (AMS, Liu et al., 2012). We averaged these data to 1 h time resolution in order to compare to the hourly CMAQ model output, which allowed for the evaluation of the ability of CMAQ to simulate the diurnal cycle of $NH_3$ concentrations. When $NH_{4(p)}$ measurements are available, we compare model results to $NH_x$ to reduce our sensitivity to gas-to-particle partitioning errors in the model; otherwise we compare to $NH_{3(g)}$.

### 2.3 TES $NH_3$ retrievals

During CalNex, TES made special observations (transects) near the Bakersfield, CA surface site with a horizontal separation of 12 km on six different afternoons. TES is a nadir-viewing Fourier-transform infrared (FTIR) spectrometer with a high spectral resolution of 0.06 $cm^{-1}$ and a nadir footprint of 5.3 km x 8.3 km. TES flies aboard the NASA Aura spacecraft, which is in a sun-synchronous orbit with an equator crossing time around 01:30 and 13:30 local solar time. Beer et al. (2008) reported the first satellite observations of boundary layer $NH_{3(g)}$ using the TES instrument. Shephard et al. (2011) developed and tested a full $NH_{3(g)}$ retrieval algorithm. The retrieval is based on an optimal estimation approach that minimizes the differences between the TES Level 1B spectra and a radiative transfer calculation that uses absorption coefficients calculated with the AER line-by-line radiative transfer model LBLRTM (Clough et al., 2006). The a priori profiles and covariance matrices for TES $NH_3$ retrievals are derived from GEOS-Chem model simulations of the 2005 global distribution of $NH_3$.

The TES $NH_{3(g)}$ retrievals generally have a region of maximum sensitivity between 700 hPa and the surface. While the retrieval is performed on 14 pressure levels, the number of degrees of freedom for signal (DOFS) is generally not greater than one. Therefore at any given single profile level the retrieved volume-mixing ratio (VMR) of $NH_3$ is highly influenced

Chantelle Lonsdale 6/21/2016 10:03 AM
**Deleted:** 1a

Chantelle Lonsdale 6/21/2016 10:03 AM
**Deleted:** 1.1

Chantelle Lonsdale 6/21/2016 10:03 AM
**Deleted:** 2014

Chantelle Lonsdale 6/21/2016 10:03 AM
**Deleted:** at a frequency of 1 Hz and

by the a priori profile. Rather than attempting to analyse data from individual retrieval levels, it is often desirable to express the retrieved information in a representation where the influence of the a priori is reduced and the information available is collapsed to a single point. To address this issue, Shephard et al. (2011) developed a Representative Volume Mixing Ratio (RVMR) metric for $NH_{3(g)}$ based on similar techniques used previously for $CH_4$ (e.g., Payne et al., 2009; Wecht et al., 2012; Alvarado et al., 2015) and $CH_3OH$ (e.g., Beer et al., 2008). This RVMR represents a TES sensitivity weighted average value where the influence of the a priori profile is reduced as much as possible; it generally ranges from 20 % to 60 % of the retrieved surface value for $NH_{3(g)}$. The minimum detection level for TES $NH_{3(g)}$ retrievals is an RVMR of approximately 0.4 ppbv, corresponding to a profile with a surface-mixing ratio of about 1-2 ppbv (Shephard et al., 2011).

Pinder et al. (2011) showed that the TES $NH_3$ retrievals were able to capture the spatial and seasonal variability of $NH_3$ over eastern North Carolina and that the retrievals compared well with in situ surface observations of $NH_3$, while Alvarado et al. (2011) showed that TES $NH_3$ retrievals can also capture the higher concentrations of $NH_3$ in forest fires in Canada. Sun et al. (2015) demonstrated that under optimal conditions (i.e., good thermal contrast and $NH_3$ amounts significantly above the TES level of detectability), TES $NH_3$ agreed very well with in situ aircraft and surface measurements taken in the California Central Valley during the DISCOVER-AQ 2013 campaign.

There are at least three issues that have to be considered when using $NH_3$ satellite profiles to evaluate model predictions: (a) the vertical resolution of the satellite profile is substantially coarser than that of the model profile; (b) the DOFS for $NH_3$ are generally less than 1.0; and (c) the retrieved satellite profile reflects the influence of the choice of a priori profile (Rodgers and Connor, 2003). Thus, in order to use these TES observations to evaluate CMAQ model predictions of the concentrations of $NH_{3(g)}$, we first interpolate the hourly CMAQ $NH_3$ profile predicted for 13:00 local solar time (expressed as the natural logarithm of the mixing ratio) to the TES pressure grid. We then apply the TES observation operator to the interpolated CMAQ $NH_3$ profile to derive a model TES profile ($\boldsymbol{x}_{\mathrm{TES}}$). Finally, we apply the sensitivity weighting to calculate the model RVMR ($CMAQ_{RVMR}$). This value represents the RVMR that would have been retrieved if (a) TES had sampled a profile identical to the CMAQ-simulated profile and (b) the retrieval errors due to jointly retrieved parameters, other model parameters, and instrument noise were negligible. The observation operator equation is

$$\boldsymbol{x_{TES}} = x_a + \mathbf{A}(\boldsymbol{x_{CMAQ}} - \boldsymbol{x_a}) \qquad (1)$$

$$CMAQ_{RVMR} = \mathbf{W} * \boldsymbol{x_{TES}} \qquad (2)$$

where $\boldsymbol{x_a}$ is a vector of the TES a priori $NH_3$ concentrations, $\mathbf{A}$ is the averaging kernel matrix, $\boldsymbol{x_{CMAQ}}$ is a vector of the interpolated CMAQ $NH_3$ values, and $\mathbf{W}$ is a weighting matrix (Rodgers and Connor, 2003; Payne et al., 2009).

### 2.4 PBL heights

Several studies have used lidar observations of aerosol profiles to determine the height of the planetary boundary layer (PBL) by identifying regions of large gradients in aerosol concentrations with height (e.g., Tucker et al., 2009; Lewis et al., 2013; Scarino et al., 2014; Hegarty et al., 2015). Scarino et al. (2014) and Tucker et al. (2009) define the mixed layer measured by the HSRL as ‘the volume of atmosphere in which aerosol chemical species emitted within the boundary layer are mixed and dispersed’. The NASA Langley Research Center (LaRC) airborne HSRL measured mixed layer heights during the CalNex campaign and the Carbonaceous Aerosol and Radiative Effects Study (Scarino et al., 2014), both of which we used in this study.

## 3 Models

### 3.1 WRF-ARW

CMAQ v5.0.2 was driven with meteorology provided by WRF ARW Version 3.5 (Skamarock and Klemp, 2008) that was configured with 3 nested domains of 36, 12, and 4 km horizontal grid spacing and 41 vertical layers. Shortwave and longwave radiation were calculated using the RRTMG radiative transfer code (Mlawer et al., 1997; Iacono et al., 2008). The YonSie University (YSU, Hong et al., 2006) non-local turbulent PBL scheme and the Noah land surface scheme (Chen and Dudhia, 2001) were used. Initial and boundary conditions for WRF were provided by the North American Regional Reanalysis (NARR, Mesinger et al*.,* 2006), which is recognized as state-of-the-science for North America (Bukovsky and Karoly, 2007). The WRF runs were 32-hour simulations initialized every 24 hours at 0000 UTC with analysis nudging of winds, temperature and humidity above the PBL on the inner 12 km domain as well as winds in the PBL as in Nehrkorn et al. (2013). The WRF outputs for UTC hours 09:00 to 32:00 from each consecutive simulation were combined to form a continuous time series and the initial 8 hours of each simulation were discarded as spin-up time. The 8-h spin-up time and 32-h simulation length is longer than the 6-h spin-up time and 30-h simulation length used by Nehrkorn et al. (2013), but were necessary to perform 24-hour daily CMAQ runs using the 24-h daily CARB emissions files that started at 8:00 UTC. The WRF output was then converted to CMAQ-model-ready files using the Meteorology-Chemistry Interface Processor version 4.2 (MCIP).

### 3.2 CMAQ

We ran CMAQ on the inner 4 km WRF domain using the SAPRC07 chemical mechanism (Hutzell et al., 2012, Carter et al., 2010ab), which corresponds to the model-ready emission files for CalNex provided by CARB, and with the CMAQ AERO6 aerosol module with aqueous chemistry. Biogenic emissions, photolysis rates, and deposition velocities were all calculated inline. There were few clouds in California during this study period and thus lightning $NO_X$ emissions were negligible; however, lightning $NO_x$ emissions were also calculated inline in CMAQ. Initial and horizontal boundary conditions for CMAQ were provided by GEOS-Chem simulations on a 2° x 2.5° latitude-longitude grid for May and June 2010 following the approach of Lapina et al. (2014).

CMAQ emissions inputs for the state of California were provided as model-ready files by CARB, which prepared them using the Modeling Emissions Data System on a 4 km x 4 km grid-scale (available at http://orthus.arb.ca.gov/calnex/data/calnex2010.html, last accessed June, 2016). The emission change log is provided at ftp://orthus.arb.ca.gov/pub/outgoing/CalNex/2010/modelready/Change Log for Posted Inventories.pdf (last accessed June, 2016). In this inventory, the $NH_3$ emissions in SJV are assumed to be constant throughout the day (i.e., no diurnal cycle), and are constant day-to-day in a given month. As the CARB model-ready files had no out-of-state emission sources, our initial simulations were run using the CARB emissions for California, the GEOS-Chem boundary conditions, and no out-of-state emissions. We quantified the potential error in gas-phase $NH_{3(g)}$, Aitken and Accumulation mode aerosol $NH_{4(p)}$, and $NH_x$ in the SJV from neglecting out-of-state agricultural $NH_3$ emissions by using the agricultural $NH_3$ emissions from the NEI2011 platform, which we re-gridded from 12 km to our model's 4 km scale while keeping California state emissions constant. We performed this sensitivity test for a 7-day case study between 25-31 May with a 4-day spin up. Adding these out-of-state emissions had a negligible impact on the modelled $NH_3$ concentrations in the SJV (less than 0.001 % change), as the prevailing winds are mostly out of the north and northwest. Additionally, we tested the effect that errors in the boundary conditions from GEOS-Chem might have on the model runs. Doubling $NH_3$ boundary conditions for the same 7-day case study also had little impact on $NH_3$ concentrations in the SJV (less than 0.001 % change), which was expected based on the short lifetime of $NH_3$.

Finally, we also ran CMAQv5.0.2 using the bi-directional $NH_3$ flux scheme as developed by Bash et al. (2013) that uses fertilizer application data, crop type, soil type, and meteorology from MCIP output to calculate soil emissions potential and $NH_4$ to simultaneously calculate $NH_3$ deposition and emission fluxes for the CMAQ US domain. This scheme uses the U. S. Department of Agriculture's Environmental Policy and Integrated Climate (EPIC) model (Cooter et al., 2012) as contained in the Fertilizer Emissions Scenario Tool (FEST-C).

### 3.3 HYSPLIT

In order to explore the sources influencing the Bakersfield concentrations we ran the HYSPLIT model. Using meteorological inputs from the WRF 4 km domain discussed in Section 3.1, we generated 36-hour back trajectories with Version 4 of the HYSPLIT model (Draxler and Hess, 1998) initiated from 100 m above ground level (agl) at Bakersfield at 17:00 PDT on June 18th back to 20:00 PDT on June 17th. Results from these runs are briefly discussed in Section 4.1.

## 4 Model Evaluation

In order to evaluate CMAQ v5.0.2 modelled $NH_3$ in the SJV we ran three different scenarios for a month long case-study that covers the record of the Bakersfield surface observations (May 22 – June 22, 2010). The model scenarios include: 1) a baseline model run ($CMAQ_{base}$), in which the model was set up as described in Section 3.2, utilizing the CARB emissions inventory; 2) $CMAQ_B$, which ran with the baseline set up but also included the bi-directional $NH_3$ scheme described in Section 3.2, and finally 3) $CMAQ_{AB}$, which included both the bi-directional $NH_3$ scheme and diurnally-varying emissions in the SJV, as described in Section 4.1. The following subsections describe the evaluations of all three model scenarios using the three different measurement datasets (surface, aircraft, and satellite) from the CalNex campaign.

Chantelle Lonsdale 6/22/2016 10:06 AM
**Deleted:** January

Chantelle Lonsdale 6/21/2016 10:03 AM
**Deleted:** $NH_3$ emissions in the SoCAB did have a strong diurnal cycle, as about 75 % of the $NH_3$ emissions were coded as "industrial" and only emitted between 8 AM and 4 PM local time. As these emissions were mainly due to sewage treatment, this diurnal cycle assumption is likely incorrect. However, evenly distributing these SoCAB emissions across the day had little impact on $NH_3$ in the SJV.

Chantelle Lonsdale 6/21/2016 10:03 AM
**Deleted:** in order to correspond to in situ measurements and two of the TES transects.

Chantelle Lonsdale 6/21/2016 10:03 AM
**Deleted:** 10

Chantelle Lonsdale 6/21/2016 10:03 AM
**Deleted:** with results discussed in Section 4.4. This tool

Chantelle Lonsdale 6/23/2016 7:11 AM
**Deleted:** ( as contained in the Fertilizer Emissions Scenario Tool (FEST-C)

Chantelle Lonsdale 6/22/2016 1:59 PM
**Deleted:** Hybrid Single-Particle Lagrangian Integrated Trajectory (

Chantelle Lonsdale 6/22/2016 2:00 PM
**Deleted:** )

Chantelle Lonsdale 6/21/2016 10:03 AM
**Deleted:** 3

### 4.1 Evaluation of modelled diurnal variability of $NH_{3(g)}$ using surface observations

Table 1 shows that the $CMAQ_{base}$ scenario has a $NH_x$ positive mean bias of 8.24 ppbv over the month-long surface data record; we focus on $NH_x$ so as to minimize the effects of possible model errors in gas-to-particle partitioning on our analysis, as discussed later in this section. However, this bias is not constant throughout the day, as can be seen in the $CMAQ_{base}$ results (blue line) shown in Figure 2. Figure 3a shows the average hourly ratio of $CMAQ_{base}$ modelled $NH_x$ versus measured concentrations for the Bakersfield ground site, averaged over all days of the CalNex campaign; these ratios are derived from the boxplots shown in Figure 3b. The model bias shows a clear diurnal cycle, with $CMAQ_{base}$ significantly overestimating surface $NH_x$ concentrations at night by up to a factor of 4.5 and generally underestimating $NH_x$ during the daytime at 0.6 between 13:00 and 14:00 local time, consistent with the average $TES_{RVMR}$ observations near Bakersfield at about 13:30 local solar time plotted as the green dot in Figure 3a and further discussed in Section 4.3. These results suggest that the constant daily emissions for agricultural $NH_3$ emissions in the CARB inventory (blue line Figure S1 in the Supplemental Material) may be misrepresenting the diurnal emission patterns suggested by the measurements. This is consistent with previous work done in North Carolina; Wu et al. (2008) found that $NH_3$ emissions from livestock feed lots show a strong diurnal cycle, peaking at mid-day.

Besides errors in emissions another contributing factor to the modelled bias of $NH_{3(g)}$ could be errors in the gas-to-particle partitioning of $NH_{3(g)}$ to $NH_{4(p)}$. Figure 2a also shows an average hourly plot of the ratio of $CMAQ_{base}$ modelled to measured $NH_x$ and $NH_{3(g)}$ during the campaign. There is very little difference between the two lines, indicating only a small fraction of total $NH_{3(g)}$ is converted into $NH_{4(p)}$ in this region, consistent with Baker et al. (2013). Thus, errors in gas-particle partitioning of $NH_3$ in CMAQ, while important for accurately estimating $PM_{2.5}$ concentrations, cannot account for the diurnal errors in $NH_x$ we have observed.

Another potential source of diurnal errors in modelled $NH_x$ are diurnal variations in meteorology, which could potentially alter the source regions to which the Bakersfield site was sensitive throughout the day. Differences in $NH_3$ emission errors at upwind sites would thus appear as diurnal errors in $NH_x$. We ran a HYSPLIT case study for June 18th, where back trajectories were run for eight different times during the day (Figure S2). As on most days during the CalNex campaign, there is a general flow from the north/north-west that is funnelled through the California Central Valley towards Bakersfield. In these simulations there is no significant change in meteorology with time of day, thus diurnal changes in transport are not likely a contributing factor to the diurnal mismatch shown in modelling results. Thus, these back trajectories, driven with our WRF model, did not show a change in source attribution locations.

Diurnal errors in the PBL height estimates could also potentially be responsible for the diurnal pattern in the CMAQ $NH_x$ concentrations at Bakersfield (Figure 3). We used daytime HSRL measurements taken in the SJV during CalNex to evaluate our WRF simulated PBL heights. Figure 4 shows 2-minute averages of the HSRL calculated mixed layer height compared to the WRF PBL for three daytime flights that passed over the SJV. The modelled and measured heights show good agreement, having a slope of 0.76, $r^2$ of 0.70, and mean bias of 87 m. Thus errors in daytime PBL height do not seem to account for much of the underestimate in modelled daytime $NH_x$. Scarino et al. (2014), when comparing all CalNex HSRL flight measurements to their configuration of the WRF-Chem model, found similar results. In summary, gas-to-particle partitioning and PBL height errors are likely not responsible for the diurnally varying measurement to model biases.

CARB $NH_3$ emissions in the SJV are constant both diurnally and day-to-day, with an hourly flux of around 0.23 moles $s^{-1}$ for the Bakersfield area (Figure S1). The Bakersfield ground measurements, however, indicate there should be a diurnal pattern of lower emissions at night and higher emissions during the day, as has been previously reported of $NH_3$ emissions from livestock (e.g., Bash et al., 2013; Zhu et al., 2015a) and other agricultural $NH_3$ sectors (Skjøth et al., 2011). We tested two methods to improve the diurnal cycle of $NH_3$ emissions in the CMAQ model. We found that including the bi-directional flux of $NH_3$ in the $CMAQ_B$ case (green lines) significantly reduces the night-time concentration peaks of $NH_3$. However there is still a clear model overestimate (mean bias of 4.57 ppb, see Table 1), with the $CMAQ_B$ scenario also causing overestimates following the day's maximum in temperature (Figure 2).

To further improve the model simulations, we applied a scaling factor to all $NH_3$ area sources per grid box in the SJV, based on the $CMAQ_{base}$ bias relative to the ground measurements. To do this, we first calculated the total $NH_3$ area source emissions for each grid box, based on additional information on the emissions breakdown from the CARB inventory. For Kern County, where Bakersfield, CA resides, pesticide/fertilizer applications dominate the $NH_3$ emissions inventory at 72%, followed by farming operations at 25%, and other sources for the remaining fraction. Table S2 in the Supplemental Material describes the fraction of $NH_3$ emissions for counties in the SJV. We then calculated the emissions for each hour based on the hourly average ground measurements. Note that the adjusted maximum emissions vary by about a factor of 4.5 from the minimum at night to the mid-day peak, as can be seen in Figure S1 (solid red line) which is more modest than the factor of 10 variation seen in livestock feedlots (Bash et al., 2013; J. Bash, personal communication, Oct. 6, 2015). We then reran CMAQ with both these adjusted emissions and the bidirectional $NH_3$ scheme (the $CMAQ_{AB}$ run) to assess the impact. Despite applying the scaling factor to all emissions instead of solely to the feedlots as in Bash et al. (2013), the $CMAQ_{AB}$ model predictions, shown as the purple lines in Figure 2, matches the measurements (black line) better than the $CARB_{base}$ or $CARB_B$ scenarios over the day and night, consistent with Bash et al. (2013), with the mean night-time bias reduced by about a factor of 2 and the overall bias reduced to -1.23 ppbv (Table 1) and does particularly well between the hours of 01:00 and 06:00. The fact that adding the diurnally-varying emission profile improves the model performance, even though the emissions are dominated by fertilizer applications that should be accounted for by the bi-directional $NH_3$ scheme, suggests that the scheme in CMAQ v5.0.2 is not correctly accounting for the diurnal variations in $NH_3$ flux in the SJV.

As noted above, the results for $NH_{3(g)}$ generally track the results for $NH_x$ already discussed. In contrast, the model usually under-predicts the small amount of $NH_{4(p)}$ observed (on average < 1 ppbv, Figure 2c) by a factor of 2, with little variation between the model scenarios (Table 1). These model errors in $NH_{4(p)}$ reflect not only model errors in total $NH_x$, but also errors in the formation of $HNO_{3(g)}$ and $SO_{4(p)}$ (Figure S3). $HNO_{3(g)}$ is overestimated in all model simulations up to a factor of 4, with concentrations not changing between model cases. $SO_{4(p)}$ measured concentrations are minimal and don't appear to have any trend and also do not change with model cases. However, as our interest in this study is in constraining $NH_3$ emissions, not inorganic aerosol formation, we do not investigate these errors further here.

### 4.2 Evaluation of modelled vertical distribution of $NH_{3(g)}$ using aircraft observations

The aircraft observations in the SJV indicate a large underestimate (range of factors about 1 to 5) in $CMAQ_{base}$ modelled $NH_x$ concentrations at higher altitudes as shown in Table 2 (all flights in SJV) and Figure 5 (two flights). The variation in model concentrations in the background of Figure 5 are due to the aircraft flying in and out of different horizontal grid boxes in the model. The May 24th flight shows a strong $CMAQ_{base}$ $NH_x$ underestimate of about a factor of 5 when considering the entire flight with an $r^2$ value of 0.31 and mean bias of -1.95 ppbv. This significant underestimate could potentially be due to an underestimate of vertical mixing at night (discussed below); when only data before 18:00 PDT is considered (assuming this is before the collapse of the convective boundary layer) the underestimate is only a factor of ~1.5 and the $r^2$ is 0.77, a considerably better result. However, model comparisons to flight data on 16 and 18 of June before 18:00 PDT, likely before the boundary layer collapse on these days, also show a significant model underestimate and low $r^2$ values; thus there may be other contributing factors to this bias. As for the surface observations, the aircraft results for $NH_x$ and $NH_{3(g)}$ are very similar. $NH_{4(p)}$ has a large absolute mean bias for all flights, but its low magnitude has a negligible effect on $NH_x$ concentrations (see Table 2).

Early afternoon (Figure 5a) and evening (Figure 5b) $CMAQ_{base}$ comparisons show a clear difference in the vertical distribution of $NH_x$. At night (May 24th flight), the model contains most of the $NH_x$ in the lowest model level, whereas during the day (June 16th flight) it vertically mixes the $NH_x$. These results could suggest 1) vertical mixing is stronger than simulated in the model during both flights, based on the higher $NH_x$ concentrations that the aircraft is measuring at higher altitudes, or 2) that there is a residual layer of $NH_x$ at night that is not captured by the model or 3) there is a non-local source that is also not well captured by the model.

Gas-phase $NH_3$ can either be deposited to or emitted from the surface depending on the land-type, land-use, and ambient concentrations (Bash et al., 2015; Fowler et al., 2009). The $CMAQ_{base}$ run does not take this into consideration, but when bi-directional $NH_3$ is calculated in $CMAQ_{AB}$ and $CMAQ_B$, $NH_3$ dry deposition should generally decrease, increasing the net land-atmosphere flux (Bash et al., 2013). Figure 5c is consistent with these results (and inconsistent with the hypothesis that vertical mixing is underestimated in the model) as the vertically distributed concentration of $NH_x$ significantly increases from the $CMAQ_{base}$ case to the $CMAQ_B$ case. The transport of $NH_3$ also tends to increase, this being a potential explanation for the plume entering the plot domain around 21:00 PDT in the bottom curtain plot. The total column concentration of $NH_x$ also increases, leading to a significant positive model bias for the $CMAQ_{AB}$ and $CMAQ_B$ scenarios (e.g. in the earlier part of the flight in Figure 5c and Table 2), suggesting a possible overestimation of total $NH_x$ emissions by the bi-directional $NH_3$ scheme during the afternoon and evening hours that the flights took place.

### 4.3 Evaluation of modelled $NH_{3(g)}$ with TES $NH_3$ retrievals

Figure 6a shows the RVMR retrieved from the TES spectra ($TES_{RVMR}$) for one overpass (during one hour of model output) on 12 May 2010; the other overpasses during the campaign are similar. Figure 6b shows the equivalent $CMAQ_{base}$ modelled $NH_3$ RVMR ($CMAQ_{RVMR}$) (see Equation 1 and 2 in Section 2.2), and Figure 6c shows the difference between the two. This figure demonstrates that the $CMAQ_{base}$ case can identify the locations of different sources of $NH_3$ and the resulting geographical relative changes in $NH_3$ along the transect, but that the $NH_3$ RVMRs are underestimated, particularly at higher $NH_3$ RVMRs (Table 3 and Table S2). Figure 7 shows the modelled and measured RVMR for four transects near Bakersfield between May 22 and June 22 (i.e., during the surface measurement record). The RVMRs for these overpasses are reasonably well correlated ($r^2$ of 0.64 and mean bias of -2.57 ppbv, Table 3), again suggesting that the $CMAQ_{base}$ inventory does a good job of capturing the spatial distribution of $NH_3$ emissions near Bakersfield. However the slope of the linear regression of $CMAQ_{base}$ RVMR suggests that CMAQ underestimates high $NH_3$ concentrations by a factor of 2.4. This demonstrates the importance of using highly time-resolved observations of $NH_3$ to determine the diurnal cycle of $NH_3$ along with polar-orbiting satellite retrievals of $NH_3$ to improve the spatial and seasonal distribution of the emissions, as noted in Zhu et al. (2013). In other words, if we had relied solely on the TES observations at 13:30 local solar time to evaluate the $CMAQ_{base}$ runs, we would have incorrectly assumed that the CARB inventory was a factor of 2.4 too low for total $NH_3$ emissions, whereas the surface data demonstrate that the problem is primarily in the diurnal cycle of the emissions.

The RVMR bias for these four overpasses changes from -2.57 ppbv to 0.84 ppbv from the $CMAQ_{base}$ run to the $CMAQ_B$ run, respectively (Table 3). The linear regression slope of the observation-model RVMR comparison also improves from 0.47 to 0.93, consistent with the results of Zhu et al. (2015a). Adding adjusted emissions (the $CMAQ_{AB}$ case) increases the RVMR bias to 1.31 ppbv, but improves the regression slope to 1.02. The absolute RVMR bias is thus still better than in the $CMAQ_{base}$ run, but is worse than in the $CMAQ_B$ case.

However, the model RVMR can be very sensitive to errors in the modelled vertical distribution of $NH_3$. We investigated this by comparing each level of the TES retrieved $NH_3$ profile with the corresponding CMAQ profile level after the observation operator is applied. Figure 8 shows box-and-whisker plots of this comparison for the $CMAQ_{base}$ and $CMAQ_{AB}$ model scenarios. This plot differs from that in Shephard et al. (2015) in that it includes the average of layers below 908 mb, which introduce an RVMR bias due to levels that are below 1000 mb. For $CMAQ_{base}$, there is a substantial negative bias in the lowest level (-5 ppb), but for $CMAQ_{AB}$ this switches to a positive, smaller bias (~1 ppb). Furthermore, the other, higher levels show little bias (~0.08 ppb). Thus comparing the TES and CMAQ profiles level-by-level indicates that the $CMAQ_{AB}$ scenario performs the best in simulating the TES retrievals, consistent with the conclusions based on the surface observations in Section 4.1.

## 5 Discussion

The results in Section 4 show that the CMAQ model scenario that included both the bi-directional $NH_3$ scheme and the diurnally adjusted emissions ($CMAQ_{AB}$) gave results that were much closer to the surface measurements (Section 4.1) and satellite (Section 4.3) observations than the $CMAQ_{base}$ runs, with measurement uncertainties explained in Section 2. The $CMAQ_{AB}$ simulations also resulted in a large overestimate of $NH_x$ concentrations higher in the atmosphere as measured by the aircraft (Section 4.2). Here we discuss the remaining errors in the $CMAQ_{AB}$ scenario, suggest possible explanations for these errors, and make suggestions for the direction of future research.

Both the night-time and daytime simulation of surface $NH_x$ is improved in the $CMAQ_{AB}$ scenario. The total bias is significantly reduced from a factor of 4.5 at night and 0.6 during the day in the $CMAQ_{base}$ scenario (Figure 3a). In $CMAQ_{AB}$, the model does a particularly better job as compared to measurements between the hours of 1:00 am and 6:00 am local time (Figure 9a), perhaps related to the lower emissions at this time of day when adjusted emissions are used. The remaining diurnal bias shows a relative model underestimate with a factor of ~0.6 at 10:00 local time and a relative model overestimate peaking at ~1.7 at 19:00 local time (Figure 9a), with average $CMAQ_{AB}$ modelled concentrations slightly higher in the afternoon and peaking around 19:00 (Figure 9b). It is interesting to note that the $CMAQ_{AB}$ bias relative to surface concentrations is small near the TES overpass time (e.g., crossing 0% between 13:00 and 14:00 local time, Figure 9a), which is consistent with the small bias seen in the comparison with the TES observations in Section 4.3. Furthermore, the aircraft results for the $CMAQ_{AB}$ scenario discussed in Section 4.2 also show a large relative overestimate in the afternoon and evening when the flights took place (Table 2), consistent with the afternoon and evening overestimates seen in the surface data.

Thus all three datasets suggest that the remaining errors in modelled $NH_x$ concentrations are due to the diurnal profile of the net land-atmosphere $NH_3$ flux in the $CMAQ_{AB}$ run peaking too late in the day. One possibility is that the diurnal cycle we applied to the non-fertilizer $NH_3$ emissions, which was based on the ambient measurements of $NH_3$, is peaking too late in the day. However, as the peak of our assumed diurnal profile for these emissions (Figure S1) is consistent with the peak in surface temperature (1:00 pm, Figure 2d), we consider this explanation less likely than remaining errors in the bi-directional $NH_3$ scheme for fertilizer emissions.

These errors in the bi-directional $NH_3$ scheme could be due to errors in the dynamic emissions response of the bi-directional $NH_3$ scheme to local temperature and wind speed conditions (Bash et al., 2013). However, Figure 2d shows that the modelled surface temperature and wind speed are not that far off from the values observed at the Bakersfield site. Thus the remaining errors are less likely related to errors in atmospheric meteorological conditions, and are more likely due to errors in the dependence of soil conditions (e.g., soil temperature, pH, and water content) on meteorology and crop management practices as calculated within the bi-directional $NH_3$ scheme (Cooter et al., 2012). The scheme calculation assumes two soil layers (0.01 m and 0.05 m) that independently exchange $NH_x$ with the canopy, which then exchanges $NH_x$ with the surface layer of the atmosphere (Bash et al., 2013). If the calculation of the response of soil properties in these layers to surface meteorology and crop management practices is incorrect (e.g., the soil layers do not heat up or cool down quickly enough with the change in surface temperature), that would affect the amount of $NH_x$ available from the soil as well as the rate at which the soil $NH_4^+$ is converted to $NO_3^-$ through nitrification (Bash et al., 2013). This would result in errors in the flux of $NH_x$ from the soil to the canopy, thus altering the canopy compensation point and the net atmospheric flux.

The aircraft results may also suggest errors in the vertical mixing of $NH_x$ during the afternoon and evening (e.g., the peak of the PBL height and the collapse). While we consider this effect as likely less important to the remaining errors in $CMAQ_{AB}$ than the potential errors in the bi-directional $NH_3$ scheme already discussed, an overestimate of vertical mixing during the afternoon would overestimate the flux of $NH_x$ from the surface layer of the atmosphere to the upper levels, consistent with the aircraft overestimate. In addition, the soil-canopy-surface atmosphere system would respond to this overestimate of vertical mixing by increasing the net flux of $NH_x$ from the soil to the atmosphere in order to maintain equilibrium, resulting in a total overestimate of the emissions of $NH_x$ during the afternoon and evening.

We thus recommend that future work to improve the simulation of atmospheric $NH_x$ concentrations in the SJV focus on bottom-up and top-down approaches that will better estimate the diurnal changes in the canopy compensation point that determines the net flux from the land to the atmosphere in the bi-directional $NH_3$ scheme (Bash et al., 2013). This scheme was originally developed using field scale observations taken in North Carolina, USA (Walker et al., 2013), so it is not surprising that this approach may need modification to work in the SJV. We recommend, first, that the CARB $NH_3$ inventory be updated to better separate $NH_3$ emissions from fertilizer and livestock. The Bash et al. (2013) scheme assumes that these two sectors will dominate the $NH_3$ emissions, while the CARB inventory divides fertilizer/pesticide use from "farming operations", and thus it is unclear if these other farming practices are dominated by livestock or not. Second, the data on crop management (e.g., fertilizer amount, timing, form, and distribution) used in EPIC (and thus in the CMAQ bi-directional $NH_3$ scheme) is based on data for the entire West Coast of the US (e.g., California, Oregon, and Washington), and thus may not be representative of farming practices in the SJV. Better crop management data specific to the SJV, as well as more SJV-specific data on soil moisture and heating rates, may thus help in removing some of the remaining errors in the $CMAQ_{AB}$ scenario. Third, in order to better connect these bottom-up emission estimates to the measured atmospheric concentrations, we recommend that top-down studies focus not just on correcting the net $NH_x$ flux to the atmosphere but also determine the diurnally-varying biases in the canopy compensation point that determines these net fluxes. This may require the development of adjoint methods and models (e.g., Zhu et al., 2015a) that can retrieve time-varying correction factors for the canopy compensation point, rather than just for the net flux itself.

## 6 Conclusions

We used $NH_3$ retrievals from the NASA Tropospheric Emission Spectrometer, as well as surface and aircraft observations of $NH_{3(g)}$ and submicron $NH_{4(p)}$ gathered during the CalNex campaign, to evaluate the ability of the CMAQ model run with the CARB emission inventory to simulate ambient $NH_{3(g)}$ and $NH_{4(p)}$ concentrations in California's San Joaquin Valley. We find that CMAQ simulations of $NH_3$ driven with the CARB inventory are qualitatively and spatially consistent with TES satellite observations, with a correlation coefficient ($r^2$) of 0.64. However, the surface observations at Bakersfield indicate a diurnally varying model bias, with $\mathrm{CMAQ}_{\mathrm{base}}$ overestimating $NH_3$ at night by at times more than 50 ppbv and underestimating it during the day by up to 10 ppbv. The surface, satellite, and aircraft observations all suggest that the afternoon $NH_3$ emissions in the CARB inventory used in $\mathrm{CMAQ}_{\mathrm{base}}$ are underestimated by at least a factor of two, while the night-time overestimate of $NH_3$ is likely due to a combination of overestimated night-time $NH_3$ emissions and underestimated night-time deposition. Thus the diurnally-constant $NH_3$ emissions used by CARB in the SJV likely misrepresent the diurnal emission cycle.

Using the bi-directional $NH_3$ scheme in CMAQ ($\mathrm{CMAQ}_{\mathrm{B}}$) resulted in reduced $NH_x$ concentrations at night and a slight increase during the day, overall reducing the model bias relative to the surface and satellite observations. However, this scenario substantially increased the simulated mixing ratio of $NH_x$ at higher altitudes, leading to an increased bias relative to the aircraft observations. In addition, errors in the simulation of the night-time surface concentrations remained in this scenario.

In order to further improve the model, we used the surface observations at Bakersfield to derive an empirical diurnal cycle of $NH_3$ emissions in the SJV in which night-time and midday emissions differed by about a factor of 4.5. Adding this diurnal profile to the CMAQ bi-directional $NH_3$ simulations ($\mathrm{CMAQ}_{\mathrm{AB}}$) while keeping the daily total $NH_3$ emissions constant at the CARB values significantly improved the model performance at night relative to the surface observations, on top of the already improved results from the $\mathrm{CMAQ}_{\mathrm{B}}$ simulations. Comparisons with the TES RVMR showed a slight increase in the bias for the $\mathrm{CMAQ}_{\mathrm{AB}}$ scenario relative to $\mathrm{CMAQ}_{\mathrm{B}}$, but further examination of the modelled and retrieved vertical profiles suggests that this is primarily due to ~1 ppb differences in the lowest retrieved level with the $\mathrm{CMAQ}_{\mathrm{AB}}$ scenario showing little bias (0.08 ppbv) relative to the TES $NH_3$ profile above this surface level. However, even in the $\mathrm{CMAQ}_{\mathrm{AB}}$ scenario sizable errors (up to 20 ppbv) in the afternoon and evening $NH_3$ remained, possibly due to the net land-atmosphere $NH_3$ flux calculated by the bi-directional $NH_3$ scheme peaking too late in the day due to errors in the calculated response of the soil conditions (e.g., soil temperature, pH, and water content) to meteorology and crop management practices.

We recommend that future work on modelling $NH_x$ emissions in the SJV include (a) updating the CARB $NH_3$ inventory to account for $NH_3$ from fertilizer, livestock, and other farming practices separately, (b) adding information on crop management practices specific to the SJV region to the EPIC-FESTC system, and (c) top-down studies that focus not just on correcting the net $NH_x$ flux to the atmosphere but also on determining the diurnally-varying biases in the canopy compensation point that determines these net fluxes.

## Acknowledgements

The authors thank Leo Ramirez and Jeremy Avise at CARB for the emissions inventory data they provided, as well as Eli Mlawer, Thomas Nehrkorn and Elizabeth Steinhubel of AER and Jesse Bash, Jim Kelly, and Kirk Baker of the EPA for their valuable comments and discussions on this work. This work was funded by the NOAA Climate Program Office Atmospheric Chemistry, Carbon Cycle, & Climate (AC4) program through Grants NA130AR4310060 and NA140AR4310129 to CRL, JDH, KCP, and MJA of AER and DKH, MDT, and SLC of CU Boulder. Development and evaluation of the TES $NH_3$ retrieval was funded through NASA grants to KCP of AER such as Grant NNH08CD52C. LMR acknowledges support from California Air Resources Board (CARB) for funding the AMS measurements (contract 09–328). Infrastructure support for the Bakersfield ground site was provided through CARB contract 08-316 to Ron C Cohen and Allen H Goldstein at the University of California, Berkeley. The collection and analysis of CalNex surface observations of $NH_{3(g)}$ at Bakersfield were funded by a University of Toronto Centre for Global Change Science award to MM and a NSERC graduate scholarship to TCV of the University of Toronto. We also wish to thank the NOAA P3 aircraft flight crew and technicians. The conclusions of this paper are the authors' only, and do not reflect NOAA or CARB policy.

## References

Alvarado, M. J., Cady-Pereira, K. E., Xiao, Y., Millet, D. B., and Payne, V. H.: Emission Ratios for Ammonia and Formic Acid and Observations of Peroxy Acetyl Nitrate (PAN) in Biomass Burning Smoke As Seen By the Tropospheric Emission Spectrometer (TES), Atmosphere, 2, 633–654, doi:10.3390/atmos2040633, 2011.

Alvarado, M. J., Payne, V. H., Cady-Pereira, K. E., Hegarty, J. D., Kulawik, S. S., Wecht, K. J., Worden, J. R., Pittman, J. V., and Wofsy, S. C.: Impacts of updated spectroscopy on thermal infrared retrievals of methane evaluated with HIPPO data, Atmos. Meas. Tech., 8, 965–985, doi:10.5194/amt-8-965-2015, 2015.

Bahreini, R., Ervens, B., Middlebrook, A. M., Warneke, C., de Gouw, J. A., DeCarlo, P. F., Jimenez, J. L., Brock, C. A., Neuman, J. A., Ryerson, T. B., Stark, H., Atlas, E., Brioude, J., Fried, A., Holloway, J. S., Peischl, J., Richter, D., Walega, J., Weibring, P., Wollney, A. G., and Fehsenfeld, F. C.: Organic aerosol formation in urban and industrial plumes near Houston and Dallas, Texas, J. Geophys. Res., 114, D00F16, doi:10.1029/2008JD011493, 2009.

Baker, K. R., Misenis, C., Obland, M. D., Ferrare, R. A., Scarino, A. J., and Kelly, J. T.: Evaluation of surface and upper air fine scale WRF meteorological modeling of the May and June 2010 CalNex period in California, Atmos. Environ., doi:10.1016/j.atmosenv.2013.08.006, 2013.

Bash, J. O., Cooter, E. J., Dennis, R. L., Walker, J. T., and Pleim, J. E.: Evaluation of a regional air-quality model with bidirectional $NH_3$ exchange coupled to an agroecosystem model, Biogeosciences, 10, 1635–1645, doi:10.5194/bg-10-1635-2013, 2013.

Bash, J., Henze, D. K., Jeong, G.-R., Zhu, L., Cady-Pereira, K. E., Shephard, M. W., Luo, M., and Pinder, R. W.: The impact of the diurnal temporal allocation of ammonia emissions on air-quality model estimates of ambient ammonia and inorganic aerosol concentrations, in preparation, 2015. 4827, 4830, 4831

Beer, R., Shephard, M. W., Kulawik, S. S., Clough, S. A., Eldering, A., Bowman, K. W., Sander, S. P., Fisher, B. M., Payne, V. H., Luo, M., Osterman, G. B., and Worden, J. R.: First satellite observations of lower tropospheric ammonia and methanol, Geophys. Res. Lett., 35, L09801, doi:10.1029/2008GL033642, 2008.

Beusen, A. H. W., Bouwman, A. F., Heuberger, P. S. C., Van Drecht, G., and Van der Hoek, K. W.: Bottom-up uncertainty estimates of global ammonia emissions from global agricultural production systems, Atmos. Environ., 42, 6067–6077, 2008.

Bricker, S., Longstaff, B., Dennison, W., Jones, A., Boicourt, K., Wicks, C., and Woerner. J.: Effects of Nutrient Enrichment In the Nation's Estuaries: A Decade of Change. NOAA Coastal Ocean Program Decision Analysis Series No. 26. National Centers for Coastal Ocean Science, Silver Spring, MD, 328 pp, 2007.

Bukovsky, M. S. and Karoly, D. J.: A brief evaluation of precipitation from the North American Regional Reanalysis, J. Hydrometeor., 8, 837–846, 2007.

Carfrae, J. A., Sheppard, L. J., Raven, J., Stein, W., Leith, I. D., Theobald, A., and Crossley, A.: Early effects of atmospheric ammonia deposition on Calluna vulgaris (L.) hull growing on an ombrotrophic peat bog, Water Air Soil Pollut. Focus, 4, 229–239, 2004.

Carmichael, G.R., Tang, Y., Kurata, G., Uno, I., Streets, D., Woo, J.-H., Huang, H., Yienger, J., Lefer, B., Shetter, R., Blake, D., Atlas, E., Fried, A., Apel, E., Eisele, F., Cantrell, C., Avery, M., Barrick, J., Sachse, G., Brune, W., Sandholm, S., Kondo, Y., Singh, H., Talbot, R., Bandy, A., Thorton, D., Clarke, A. and Heikes, B. (2003). Regional-scale chemical transport modeling in support of the analysis of observations obtained during the TRACE-P experiment. Journal of Geophysical Research 108: doi: 10.1029/2002JD003117. issn: 0148-0227.

Carter, W. P. L.: Development of the SAPRC-07 chemical mechanism, Atmos. Environ., 44, 5324–5335, 2010a.

Carter, W. P. L.: Development of a condensed SAPRC-07 chemical mechanism, Atmos. Environ., 44, 5336–5345, 2010b.

Chen, F. and Dudhia, J.: Coupling an advanced land-surface–hydrology model with the Penn State–NCAR MM5 modeling system. Part I: Model implementation and sensitivity, Mon. Wea. Rev., 129, 569–586, 2001.

Clarisse, L., Coheur, P.-F., Prata, F., Hadji-Lazaro, J., Hurtmans, D., and Clerbaux, C.: A unified approach to infrared aerosol remote sensing and type specification, Atmos. Chem. Phys., 13, 2195-2221, doi:10.5194/acp-13-2195-2013, 2013.

Clough, S. A., Shephard, M. W., Worden, J., Brown, P. D., Worden, H. M., Mingzhao, L., Rodgers, C. D., Rinsland, C.P., Goldman, A., Brown, L., Kulawik, S. S., Eldering, A., Lampel, M., Osterman, G., Beer, R., Bowman, K., Cady-Pereira, K. E., and Mlawer, E. J.: Forward Model and Jacobians for Tropospheric Emission Spectrometer Retrievals, IEEE Trans. Geosci. Remote Sens., 44, 1308–1323, 2006.

Cooter, E. J., Bash, J. O., Benson, V., and Ran, L.: Linking agri- cultural crop management and air quality models for regional to national-scale nitrogen assessments, Biogeosciences Discuss., 9, 6095–6127, doi:10.5194/bgd-9-6095-2012, 2012.

Draxler, R. R. and. Hess, G. D.: An overview of the HYSPLIT_4 modeling system for trajectories, dispersion, and deposition, Aust. Meteorol. Mag., 47, 295–308, 1998.

Ellis, R. A., Murphy, J. G, Pattey, E., van Haarlem, R., O'Brien, J. M., and Herndon, S. C.: Characterizing a Quantum Cascade Tunable Infrared Laser Differential Absorption Spectrometer (QC-TILDAS) for measurements of atmospheric ammonia, Atmos. Meas. Tech., 3, 397–406, 2010.

Ellis, R. A., Murphy, J. G., Markovic, M. Z., VandenBoer, T. C., Makar, P. A., Brook, J., and Mihele, C.: The influence of gas-particle partitioning and surface-atmosphere exchange on ammonia during BAQS-Met, Atmos. Chem. Phys., 11, 133–145, doi:10.5194/acp-11-133-2011, 2011.

Fowler, D., Pilegaard, K., Sutton, M., Ambus, P., Raivonen, M., Duyzer, J., Simpson, D., Fagerli, H., Fuzzi, S., Schjoerring, J., Granier, C., Neftel, A., Isaksen, I., Laj, P., Maione, M., Monks, P., Burkhardt, J., Daemmgen, U., Neirynck, J., Personne, E., Wichink-Kruit, R., Butterbach-Bahl, K., Flechard, C., Tuovinen, J., Coyle, M., Gerosa, G., Loubet, B., Altimir, N., Gruenhage, L., Ammann, C., Cieslik, S., Paoletti, E., Mikkelsen, T., Ro-Poulsen, H., Cellier, P., Cape, J., Horvath, L., Loreto, F., Niinemets, U., Palmer, P., Rinne, J., Misztal, P., Nemitz, E., Nilsson, D., Pryor, S., Gallagher, M., Vesala, T., Skiba, U., Brueggemann, N., Zechmeister-Boltenstern, S., Williams, J., O'Dowd, C., Facchini, M., de Leeuw, G., Flossman, A., Chaumerliac, N., and Erisman, J.: Atmospheric composition change: Ecosystems-Atmosphere interactions, Atmos. Environ., 43, 5193–5267, doi:10.1016/j.atmosenv.2009.07.068, 2009.

Galloway, J. N., Townsend, A. R., Erisman, J. W., Bekunda, M., Cai, Z., Freney, J. R., Martinelli, L. A., Seitzinger, S. P., and Sutton, M. A.: Transformation of the Nitrogen Cycle: Recent Trends, Questions, and Potential Solutions, Science, 320, 889– 892, 2008.

Gilliland, A. B., Dennis, R. L., Roselle, S. J., and Pierce, T. E.: Seasonal NH3 emission estimates for the eastern United States based on ammonium wet concentrations and an inverse modeling method, J. Geophys. Res., 108, D15, 4477, doi:10.1029/2002jd003063, 2003.

Gilliland, A. B., Wyat Appel, K., Pinder, R. W., and Dennis, R. L.: Seasonal NH3 emissions for the continental United States: Inverse model estimation and evaluation, Atmos. Environ., 40, 4986–4998, 2006.

Heald, C. L., Collett Jr., J. L., Lee, T., Benedict, K. B., Schwandner, F. M., Li, Y., Clarisse, L., Hurtmans, D. R., Van Damme, M., Clerbaux, C., Coheur, P.-F., Philip, S., Martin, R. V., and Pye, H. O. T.: Atmospheric ammonia and particulate inorganic nitrogen over the United States, Atmos. Chem. Phys., 12, 10295–10312, doi:10.5194/acp-12-10295-2012, 2012.

Hegarty, J., Henderson, J., Lewis, J., McGrath-Spangler, E., Scarino, A. J., Ferrare, R., P. DeCola, P., and Welton, E.: Evaluating High-Resolution WRF Simulations of PBL Depth Using Observations from DISCOVER-AQ 2011, Meteorology and Climate – Modeling for Air Quality, September 16-18, 2015, Sacramento, CA, 2015.

Hensen, A., Loubet, B., Mosquera, J., van den Bulk, W. C. M., Erisman, J. W., Dämmgen, U., Milford, C., Löpmeier, F. J., Cellier, P., Mikuška, P., and Sutton, M.A.: Estimation of $NH_3$ emissions from a naturally ventilated livestock farm using local-scale atmospheric dispersion modelling, *Biogeosciences,* 6, 2847–2860, 10.5194/bg-6-2847-2009, 2009.

Henze, D. K., Seinfeld, J. H., and Shindell, D. T.: Inverse modeling and mapping US air quality influences of inorganic PM2.5 precursor emissions using the adjoint of GEOS-Chem, Atmos. Chem. Phys., 9, 5877–5903, 2009.

Hong, S.-Y., Noh, Y., and Dudhia, J.: A new vertical diffusion package with an explicit treatment of entrainment processes, Mon. Wea. Rev., 134, 2318–2341, 2006.

Hristov, A. N., Hanigan, M., Cole, A., Todd, R., McAllister, T. A., Ndegwa, P. M., and Rotz, A.: Review: Ammonia emissions from dairy farms and beef feedlots, Can. J. Anim. Sci., 91(1), 1–35, doi:10.4141/CJAS10034, 2011.

Hutzell, W. T., Luecken, D. J., Appel, K. W., and Carter, W. P. L.: Interpreting predictions from the SAPRC07 mechanism based on regional and continental simulations, Atmos. Environ., 46, 417– 429, 2012.

Iacono, M. J., Delamere, J. S., Mlawer, E. J., Shephard, M. W., Clough, S. A., and Collins, W. D: Radiative forcing by long-lived greenhouse gases: Calculations with the AER radiative transfer models, J. Geophys. Res., 113, D13103, 2008.

Kelly, J. T., Baker, K. B., Nowak, J. B., Murphy, J. G., Markovic, M. Z., VandenBoer, T. C., Ellis, R. A., Neuman, J. A., Weber, R. J., Roberts, J. M., Veres, P. R., de Gouw, J. A., Beaver, M. R., Newman, S., and Misenis, C.: Fine-scale simulation of ammonium and nitrate over the South Coast Air Basin and San Joaquin Valley of California during CalNex-2010, J. Geophys. Res. Atmos., 119(6), 3600–3614. ISSN 2169-897X. 2014.

Langford, A. O., Fehsenfeld, F. C., Zachariassen, J., and Schimel, D. S.: Gaseous ammonia fluxes and background concentrations in terrestrial ecosystems of the United States, Global Biogeochem. Cy., 6, 459–483, 1992.

Lapina, K., Henze, D. K., Milford, J. B., Huang, M., Lin, M., Fiore, A. M., Carmichael, G., Pfister, G., and Bowman, K.: Assessment of source contributions to seasonal vegetative exposure to ozone in the U.S., J. Geophys. Res. Atmos., 119, 324–340, doi:10.1002/2013JD020905, 2014.

Lewis, J. R., E. J. Welton, A. M. Molod, and E. Joseph: Improved boundary layer depth retrievals from MPLNET, J. Geophys. Res. Atmos., 118, 9870–9879, doi:10.1002/jgrd.50570, 2013.

Liu, S., L. Ahlm, D.A. Day, L.M. Russell, Y.L. Zhao, D.R. Gentner, R.J. Weber, A.H. Goldstein, M. Jaoui, J.H. Offenberg, T.E. Kleindienst, C. Rubitschun, J.D. Surratt, R.J. Sheesley, and S. Scheller, Secondary Organic Aerosol Formation from Fossil Fuel Sources Contribute Majority of Summertime Organic Mass at Bakersfield, Journal of Geophysical Research – Atmospheres, 117: doi:10.1029/2012jd018170, 2012.

Lonsdale, C. R., Stevens, R. G., Brock, C. A., Makar, P. A., Knipping, E. M., and Pierce, J. R.: The effect of coal-fired power-plant $SO_2$ and $NO_X$ control technologies on aerosol nucleation in the source plumes, Atmos. Chem. Phys., 12, 2012, doi:10.5194/acp-12-11519-2012.

Markovic, M. Z., VandenBoer, T. C., and Murphy, J. G.: Characterization and optimization of an online system for the simultaneous measurement of atmospheric water-soluble constituents in the gas and particle phases, J. Environ. Monit., 14, 1872–1884, 2012.

Markovic, M. Z., T. C. VandenBoer, K. R. Baker, J. T. Kelly, and J. G. Murphy, Measurements and modeling of the inorganic chemical composition of fine particulate matter and associated precursor gases in California's San Joaquin Valley during CalNex 2010, J. Geophys. Res. Atmos., 119, doi:10.1002/ 2013JD021408.

Martin, S. T., Hung, H.-M., Park, R. J., Jacob, D. J., Spurr, R. J. D., Chance, K. V., and Chin, M.: Effects of the physical state of tropospheric ammonium-sulfate-nitrate particles on global aerosol direct radiative forcing, Atmos. Chem. Phys., 4, 183–214, doi:10.5194/acp-4-183-2004, 2004.

Mesinger, F., DiMego, G., Kalnay, E., Mitchell, K., Shafran, P. C., Ebisuzaki, W., Jovic, D., Woollen, J., Rogers, E., and Berbery, E. H.: North American regional reanalysis, B. Am. Meteorol. Soc., 87, 343–360, 2006.

Mlawer, E. J., Taubman, S. J., Brown, P. D., Iacono, M. J., and Clough, S. A.: RRTM, a validated correlated-k model for the longwave, J. Geophys. Res., 102, 16663–16682, 1997.

Moss, R. H., Edmonds, J. A., Hibbard, K. A., Manning, M. R., Rose, S. K., van Vuuren, D. P., Carter, T. R., Emori, S., Kainuma, M., Kram, T., Meehl, G. A., Mitchell, J. F. B., Nakicenovic, N., Riahi, K., Smith, S. J., Stouffer, R. J., Thomson, A. M., Weyant, J. P., and Wilbanks, T. J.: The next generation of scenarios for climate change research and assessment, Nature, 463, 747–756, doi:10.1038/nature08823, 2010.

Nehrkorn, T., Henderson, J., Leidner, M., M. Mountain, J. Eluszkiewicz, K. McKain, and S. C. Wofsy: WRF simulations of the urban circulation in the Salt Lake City area for $CO_2$ modeling, J. Appl. Meteor. Clim., 52, 323–340, 2013.

Nemitz, E., Milford, C., and Sutton, M. A.: A two-layer canopy compensation point model for describing bi-directional biosphere-atmosphere exchange of ammonia, Q. J. Roy. Meteor. Soc., 127, 815–833, 2001.

Nowak, J.B. et al., A Chemical Ionization Mass Spectrometry Technique for Airborne Measurements of Ammonia, J. Geophys. Res., 112, D10S02, doi:10.1029/2006JD007589, 2007.

Nowak, J. B., Neuman, J. A., Bahreini, R., Brock, C. A., Middlebrook, A. M., Wollny, A. G., Holloway, J. S., Peischl, J., Ryerson, T. B., and Fehsenfeld, F. C.: Airborne observations of ammonia and ammonium nitrate formation over Houston, Texas, J. Geophys. Res., 115, D22304, doi:10.1029/2010JD01495, 2010.

Nowak, J. B., Neuman, J. A., Bahreini, R., Middlebrook, A. M., Holloway, J. S., McKeen, S. A., Parrish, D. D., Ryerson, T. B., and Trainer, M.: Ammonia sources in the California South Coast Air Basin and their impact on ammonium nitrate formation, Geophys. Res. Lett., 39, L07804, doi:1029/2012GL051197, 2012.

Paulot, F. and Jacob, D. J.: Hidden Cost of U.S. Agricultural Exports: Particulate Matter from Ammonia Emissions, Environ. Sci. Technol., 48(2), 903–8, doi: 10.1021/es4034793, 2014.

Payne, V. H., Clough, S. A., Shephard, M. W., Nassar, R., and Logan, J. A.: Information-centered representation of retrievals with limited degrees of freedom for signal: Application to methane from the Tropospheric Emission Spectrometer, J. Geophys. Res., 114, D10307, doi:10.1029/2008JD010155, 2009.

Pinder, R. W., Walker, J. T., Bash, J. O., Cady-Pereira, K. E., Henze, D. K., Luo, M., Osterman, G. B., and Shephard, M. W.: Quantifying spatial and seasonal variability in atmospheric ammonia with in situ and space-based observations, Geophys. Res. Lett., 38, L04802, doi:10.1029/2010GL046146, 2011.

Pope, C. A., Burnett, R. T., Thurston, G. D., Thun, M. J., Calle, E. E., Krewski, D., and Godleski, J. J.: Cardiovascular Mortality and Year-round Exposure to Particulate Air Pollution: epidemiological evidence of general pathophysiological pathways of disease, Circulation, 109, 71–77, 2004.

RoTAP: Review of Transboundary Air Pollution: Acidification, Eutrophication, Ground Level Ozone and Heave Metals in the UK. Contract Report to the Department for Environment, Food and Rural Affairs. Centre for Ecology & Hydrology, 2012.

Rodgers, C. D. and Connor, B. J.: Intercomparison of remote sounding instruments, J. Geophys. Res., 108, doi:10.1029/2002JD002299, 2003.

Ryerson, T. B., Andrews, A. E., Angevine, W. M., Bates, T. S., Brock, C. A., Cairns, B., Cohen, R. C., Cooper, O. R., de Gouw, J. A., Fehsenfeld, F. C., Ferrare, R. A., Fischer, M. L., Flagan, R. C., Goldstein, A. H., Hair, J. W., Hardesty, R. M., Hostetler, C. A., Jimenez, J. L., Langford, A. O., McCauley, E., McKeen, S. A., Molina, L. T., Nenes, A., Oltmans, S. J., Parrish, D. D., Pederson, J. R., Pierce, R. B., Prather, K., Quinn, P. K., Seinfeld, J. H., Senff, C. J., Sorooshian, A., Stutz, J., Surratt, J. D., Trainer, M., Volkamer, R., Williams, E. J., and Wofsy, S. C: The 2010 California Research at the Nexus of Air Quality and Climate Change (CalNex) field study, J. Geophys. Res. Atmos., 118, 5830–5866, doi:10.1002/jgrd.50331, 2013.

Sawycky, M., Boulton, J. W., Trask, T., Van Heyst, B., and McClellan, C.: BC Agricultural Air Emissions Inventory. Rep. No. 1302423. Vancouver: RWDI, 2014, BC Ministry of Agriculture, 2014.

Scarino, A. J., Obland, M. D., Fast, J. D., Burton, S. P., Ferrare, R. A., Hostetler, C. A., Berg, L. K., Lefer, B. L., Haman, C. L., Rogers, R. R., Butler, C. F., Cook, A. L., and Harper, D. B.: Comparison of mixed layer heights from airborne high spectral resolution lidar, ground-based measurements, and the WRF-Chem model during CalNex and CARES, Atmos. Chem. Phys., 14, 5547–5560, doi:10.5194/acp-14-5547-2014, 2014.

Schiferl, L. D., Heald, C. L., Nowak, J. B., Holloway, J. S., Neuman, J. A., Bahreini, R., Pollack, I. B., Ryerson, T. B., Wiedinmyer, C., and Murphy, J. G.: An investigation of ammonia and inorganic particulate matter in California during the CalNex campaign, J. Geophys. Res. Atmos., 119, 1883–1902, doi:10.1002/2013JD020765, 2014.

Schlesinger, W.H., 2009. On the fate of anthropogenic nitrogen. Proceedings of the National Academy of Sciences, U.S 106, 203e208.

Shephard, M. W., Cady-Pereira, K. E., Luo, M., Henze, D. K., Pinder, R. W., Walker, J. T., Rinsland, C. P., Bash, J. O., Zhu, L., Payne, V. H., and Clarisse, L.: TES ammonia retrieval 25 strategy and global observations of the spatial and seasonal variability of ammonia, Atmos. Chem. Phys., 11, 10743–10763, doi:10.5194/acp-11-10743-2011, 2011.

Shephard, M. W. and Cady-Pereira, K. E.: Cross-track Infrared Sounder (CrIS) satellite measurements of tropospheric ammonia, Atmos. Meas. Tech., 8, 1323–1336, 2015 www.atmos-meas-tech.net/8/1323/2015/ doi:10.5194/amt-8-1323-2015, 2015.

Shephard, M. W., McLinden, C. A., Cady-Pereira, K. E., Luo, M., Moussa, S. G., Leithead, A., Liggio, J., Staebler, R. M., Akingunola, A., Makar, P., Lehr, P., Zhang, J., Henze, D. K., Millet, D. B., Bash, J. O., Zhu, L., Wells, K. C., Capps, S. L., Chaliyakunnel, S., Gordon, M., Hayden, K., Brook, J. R., Wolde, M., and Li, S.-M.: Tropospheric Emission Spectrometer (TES) satellite observations of ammonia, methanol, formic acid, and carbon monoxide over the Canadian oil sands: validation and model evaluation, Atmos. Meas. Tech., 8, 5189-5211, doi:10.5194/amt-8-5189-2015, 2015.

Simon, H., Allen, D. T., and Wittig, A. E.: Fine particulate matter emissions inventories: Comparisons of emissions estimates with observations from recent field programs, J. Air & Waste Manage. Assoc., 58, 320–343, 2008.

Skamarock, W. C. and Klemp, J. B.: A time-split nonhydrostatic atmospheric model for weather research and forecasting applications, J. Comp. Phys., 227, 3465–3485, 2008.

Skjøth, C. A., Geels, C., Berge, H., Gyldenkærne, S., Fagerli, H., Ellermann, T., Frohn, L. M., Christensen, J., Hansen, K. M., Hansen, K., and Hertel, O.: Spatial and temporal variations in ammonia emissions – a freely accessible model code for Europe, Atmos. Chem. Phys., 11, 5221-5236, doi:10.5194/acp-11-5221-2011, 2011.

Skjøth, C. A. and Geels, C.: The effect of climate and climate change on ammonia emissions in Europe, Atmos. Chem. Phys., 13, 117-128, doi:10.5194/acp-13-117-2013, 2013.

Sun, K., Cady-Pereira, K., Miller, D. J., Tao, L., Zondlo, M. A., Nowak, J. B., Neuman, J. A., Mikoviny, T., Müller, M., Wisthaler, A., Scarino, A. J., and Hostetler, C. A.: Validation of TES ammonia observations at the single pixel scale in the San Joaquin Valley during DISCOVER-AQ, J. Geophys. Res. Atmos., 120, 5140–5154. doi: 10.1002/2014JD022846., 2015.

Tucker, S. C., Brewer, Wm. A., Banta, R. M., Senff, C. J., Sandberg, S. P., Law, D. C., Weickmann, A., and Hardesty, R. M. :Doppler lidar estimation of mixing height using turbulence, shear, and aerosol profiles, J. Atmos. Ocean Tech., 26, 673–688, 2009.

Van Damme, M., Clarisse, L., Heald, C. L., Hurtmans, D., Ngadi, Y., Clerbaux, C., Dolman, A. J., Erisman, J. W., and Coheur, P. F.: Global distributions, time series and error characterization of atmospheric ammonia (NH3) from IASI satellite observations, Atmos. Chem. Phys., 14, 2905–2922, doi:10.5194/acp-14-2905-2014, 2014.

Walker, J. M., Seinfeld, J. H., Clarisse, L., Coheur, P.-F., Clerbaux, C., and Van Damme, M.: Simulation of nitrate, sulfate, and ammonium aerosols over the United States, Atmos. Chem. Phys. Discuss., 12, 19499–19527, doi:10.5194/acpd-12-19499- 2012, 2012.

Walker, J. T., Jones, M. R., Bash, J. O., Myles, L., Meyers, T., Schwede, D., Herrick, J., Nemitz, E., and Robarge, W.: Processes of ammonia air–surface exchange in a fertilized *Zea mays* canopy, Biogeosciences, 10, 981–998, doi:10.5194/bg-10-981-2013, 2013.

Wecht, K. J., Jacob, D. J., Wofsy, S. C., Kort, E. A., Worden, J. R., Kulawik, S. S., Henze, D. K., Kopacz, M., and Payne, V. H.: Validation of TES methane with HIPPO aircraft observations: implications for inverse modeling of methane sources, Atmos. Chem. Phys., 12, 1823–1832, doi:10.5194/acp-12-1823-2012, 2012.

Wichink Kruit, R. J., Schaap, M., Sauter, F. J., van Zanten, M. C., and van Pul, W. A. J.: Modeling the distribution of ammonia across Europe including bi-directional surface–atmosphere exchange, Biogeosciences, 9, 5261-5277, doi:10.5194/bg-9-5261-2012, 2012.

World Health Organization, Health Effects of Particulate Matter, Europe, available at: http://www.euro.who.int/__data/assets/pdf_file/0006/189051/, last accessed: January 2016.

Wu, S-Y., Hub, J.-L., Zhang, Y., and Aneja, V. P.: Modeling atmospheric transport and fate of ammonia in North Carolina—Part II: Effect of ammonia emissions on fine particulate matter formation, Atmos. Environ., 42, 3437–3451, 2008.

Chantelle Lonsdale 6/22/2016 12:33 PM

**Deleted:** US Environmental Protection Agency: Our Nation's Air – Status and Trends through 2008, Washington, DC, 2010.

Zhang, L., Wright, P. L., and Asman, W. A. H.: Bi-directional air-surface exchange of atmospheric ammonia – A review of measurements and a development of a big-leaf model for applications in regional-scale air-quality models, J. Geophys. Res., 115, D20310, doi:10.1029/2009JD013589, 2010.

Zhu, L., Henze, D. K., Cady-Pereira, K. E., Shephard, M. W., Luo, M., Pinder, R. W., Bash, J. O., and Jeong, G. R.: Constraining U.S. ammonia emissions using TES remote sensing observations and the GEOS-Chem adjoint model, J. Geophys. Res. Atmos., 118, 3355–3368, doi:10.1002/jgrd.50166, 2013.

Zhu, L., Henze, D., Bash, J., Jeong, G.-R., Cady-Pereira, K., Shephard, M., Luo, M., Paulot, F., and Capps, S.: Global evaluation of ammonia bi-directional exchange, Atmos. Chem. Phys. Discuss., 15, 4823–4877, doi:10.5194/acpd-15-4823-2015, 2015a.

Zhu, L., D. K. Henze, J. O. Bash, K. E. Cady-Pereira, M. W. Shephard, M. Luo, and S. L. Capps: Sources and impacts of atmospheric NH3: Current understanding and frontiers for modeling, measurements, and remote sensing in North America, Current Pollution Reports, 1(2), 95–116, 2015b.

Table 1. Summary statistics of the modelled $NH_x$, $NH_{3(g)}$ and $NH_{4(p)}$ concentration comparisons to the ground measurements for all three model runs.

| | NHx | | | | $NH_{3(g)}$ | | $NH_{4(p)}$ | |
|---|---|---|---|---|---|---|---|---|
| Model Run | Slope | $r^2$ | MB (ppbv) | MNB (%) | MB (ppbv) | MNB (%) | MB (ppbv) | MNB (%) |
| CMAQ$_{base}$ | -2.49+/-0.15 | 0.001 | 8.24 | 72.54 | 8.63 | 78.79 | -0.40 | -52.96 |
| CMAQ$_{B}$ | 1.22+/-0.07 | 0.01 | 4.57 | 45.74 | 4.99 | 50.60 | -0.41 | -55.92 |
| CMAQ$_{AB}$ | 0.85+/-0.05 | 0.05 | -1.23 | -10.70 | -0.79 | -14.01 | -0.44 | -60.24 |

Table 2. Summary statistics of the modelled to measured $NH_x$ concentration comparisons following the SJV flights.

| | | **$NH_x$** | | | | **$NH_{3(g)}$** | | **$NH_{4(p)}$** | |
|---|---|---|---|---|---|---|---|---|---|
| **Date** | **Time (PDT)** | **Slope** | **$r^2$** | **MB (ppbv)** | **MNB (%)** | **MB (ppbv)** | **MNB (%)** | **MB (ppbv)** | **MNB (%)** |
| CMAQ$_{base}$ | | | | | | | | | |
| 20100524 | 16:00-22:00 | 0.20+/-0.01 | 0.31 | -1.95 | -2.010 | -1.74 | -18.24 | -0.14 | -58.70 |
| | 16:00-18:00 | 0.68+/-0.05 | 0.77 | -0.20 | -10.79 | -0.04 | -32.46 | -0.08 | -53.19 |
| | 18:00-22:00 | 0.18+/-0.01 | 0.29 | -2.40 | -0.213 | -2.24 | -14.65 | -0.14 | -60.10 |
| 20100616 | 13:00-18:00 | 0.30+/-0.02 | 0.43 | -5.92 | -8.980 | -4.90 | -3.59 | -0.24 | -45.32 |
| 20100618 | 13:00-18:00 | 0.18+/-0.02 | 0.10 | -8.12 | -18.97 | -7.85 | -28.9 | -0.26 | -75.20 |
| CMAQ$_{B}$ | | | | | | | | | |
| 20100524 | 16:00-22:00 | 0.36+/-0.03 | 0.09 | 5.56 | 351.82 | 5.71 | 453.86 | -0.10 | -39.32 |
| | 16:00-18:00 | -1.57+/-0.24 | 0.19 | 6.59 | 506.18 | 6.71 | 639.07 | -0.07 | -31.92 |
| | 18:00-22:00 | 0.31+/-0.03 | 0.11 | 5.30 | 31.28 | 5.46 | 407.1 | -0.11 | -41.18 |
| 20100616 | 13:00-18:00 | 0.76+/-0.06 | 0.04 | 6.27 | 248.03 | 6.63 | 279.85 | -0.22 | -33.82 |
| 20100618 | 13:00-18:00 | 0.37+-0.04 | 0.02 | 4.26 | 394.88 | 4.41 | 458.88 | -0.21 | -52.37 |
| CMAQ$_{AB}$ | | | | | | | | | |
| 20100524 | 16:00-22:00 | 0.38+/-0.03 | 0.17 | 6.15 | 369.73 | 6.30 | 474.89 | -0.10 | -38.48 |
| | 16:00-18:00 | -1.61+/-0.25 | 0.16 | 6.94 | 526.88 | 7.07 | 664.26 | -0.07 | -31.17 |
| | 18:00-22:00 | 0.32+/-0.02 | 0.22 | 5.95 | 330.05 | 6.10 | 427.07 | -0.11 | -40.33 |
| 20100616 | 13:00-18:00 | 0.80+/-0.06 | 0.10 | 7.83 | 264.1 | 8.19 | 297.58 | -0.22 | -33.83 |
| 20100618 | 13:00-18:00 | 0.42+/-.05 | 0.03 | 5.59 | 425.7 | 5.76 | 494.16 | -0.21 | -50.36 |

Table 3. Summary statistics of the $CMAQ_{RVMR}$ to $TES_{RVMR}$ $NH_3$ comparisons for 4 CalNex overpasses (05/28, 05/30, 06/13, 06/15).

| **Model Run** | **Slope** | **$r^2$** | **MB (ppbv)** | **MNB (%)** |
|---|---|---|---|---|
| $CMAQ_{base}$ | 0.47 | 0.64 | -2.57 | -30.21 |
| $CMAQ_B$ | 0.93 | 0.60 | 0.84 | 14.40 |
| $CMAQ_{AB}$ | 1.02 | 0.60 | 1.31 | 19.57 |

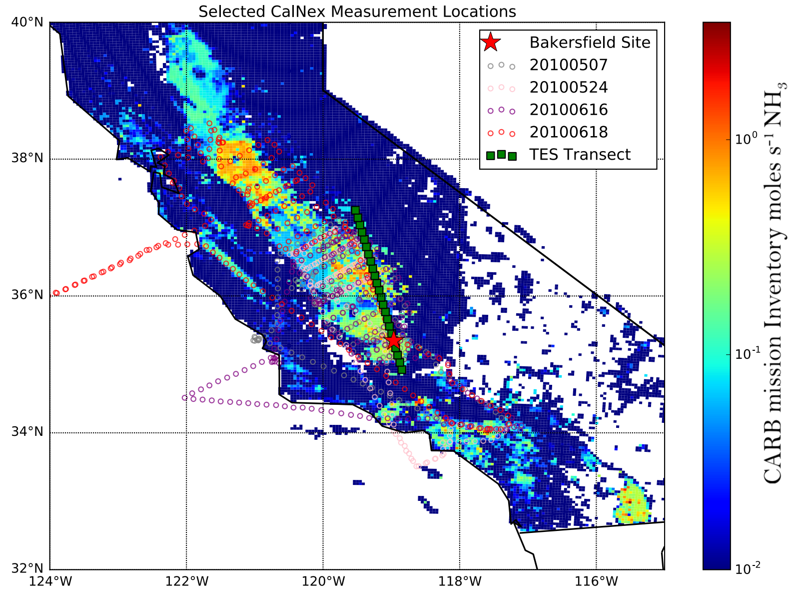

Figure 1. Distribution of $NH_3$ emissions across California (background) on May 12, 2010 at 19:00 UTC as well as P3 flight tracks (small circles), TES transect (green squares), and the Bakersfield site (red star)

Chantelle Lonsdale 6/21/2016 10:03 AM

**Deleted:** Page Break

... [1]

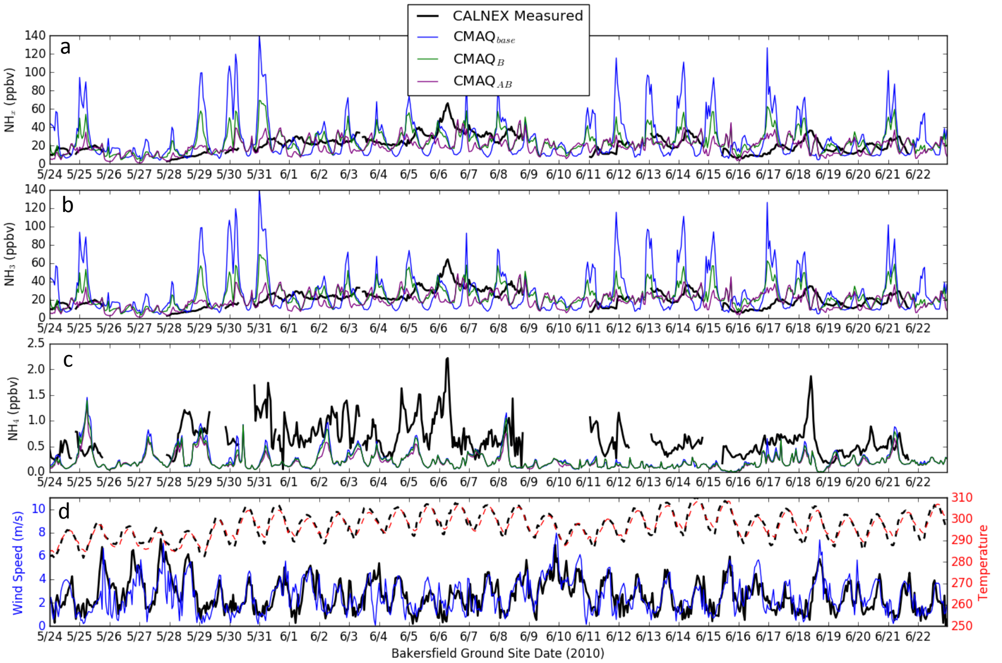

Figure 2. The CalNex ground measurements at the Bakersfield site (solid black) compared to the CMAQ$_{base}$ (solid blue), CMAQ$_{AB}$ (purple) and CMAQ$_{B}$ (green) simulations for a month of model runs. The top panel (a) shows NH$_x$, b) shows NH$_{3(g)}$, c) NH$_{4(p)}$, and d) wind speed on the left and temperature on the right axis.

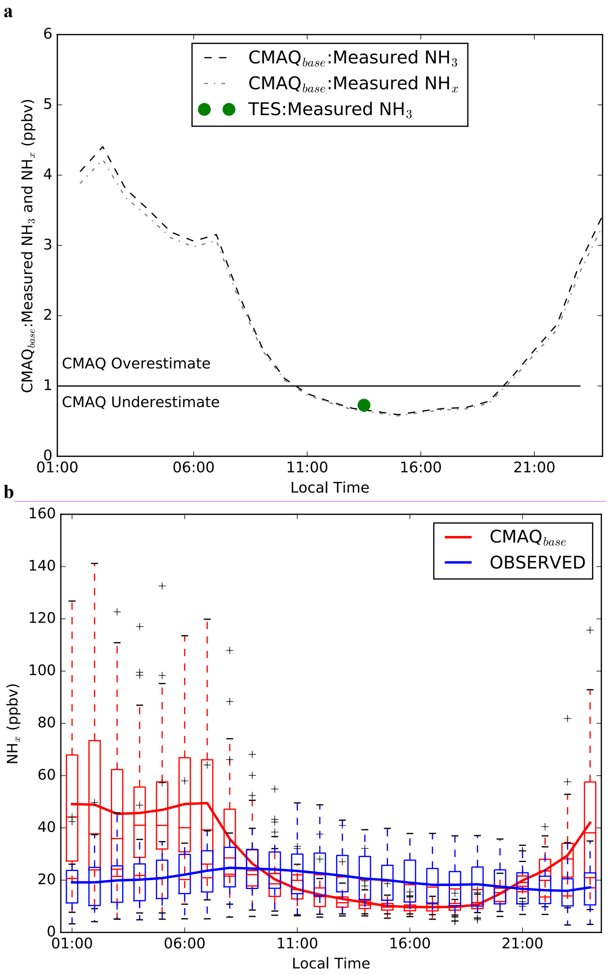

Figure 3. a) The average hourly ratio of modelled to measured $NH_3$ (dashed-dotted line) and $NH_x$ (dashed line) mixing ratios at the Bakersfield ground site and the average modelled RVMR to TES RVMR ratio (green dot) in local PDT. b) Boxplot of average hourly modelled (red) and measured (blue) $NH_x$ mixing ratios for the Bakersfield ground site, averaged over all measurement days during CalNex where the boxplots show the inter-quartile range and median line within the box and outliers (whiskers).

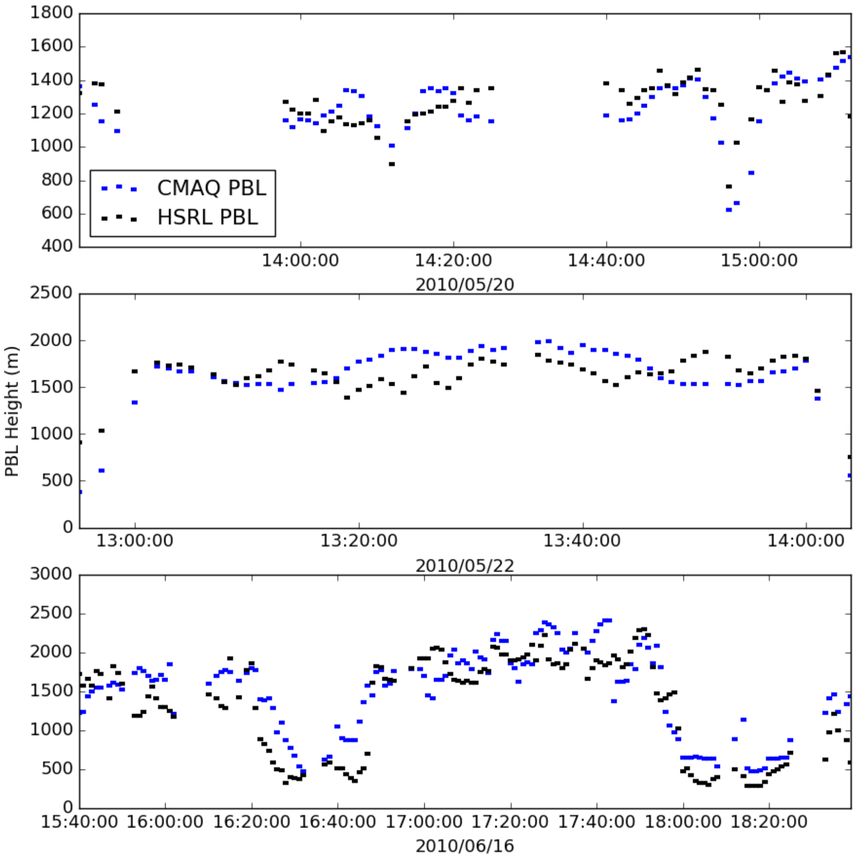

Figure 4. Time series of WRF predicted planetary boundary layer heights and HSRL calculated mixed layer heights for 3 flight sections in the San Joaquin Valley (2 during CalNex and one during a CARES campaign). 5

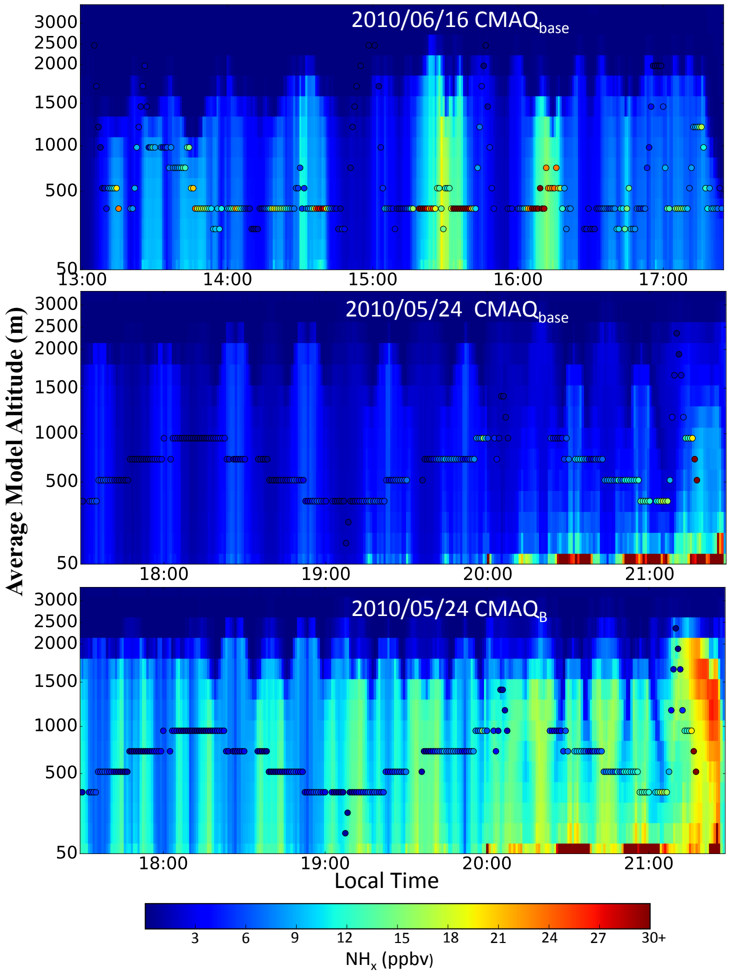

Figure 5. The hourly output of CMAQ$_{base}$ NH$_x$ is shown in the background with the measured (one minute average) NH$_x$ concentrations within the modelled hour shown as the dots. (a) Daytime flight over Bakersfield on June 16, (b) evening flight on May 24, 2010 and (c) the same as (b) but for a CMAQ$_B$ run.

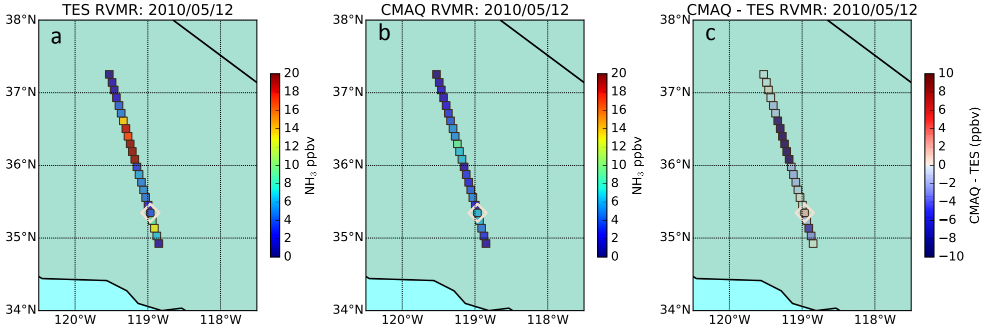

Figure 6. $NH_3$ representative volume mixing ratios (RVMRs) on 12 May 2010 during the CALNEX campaign for (a) TES special observations, (b) modelled RVMR for CMAQ and (c) the difference between each RVMR near the Bakersfield, CA, surface site with the white diamond locating the Bakersfield measurement site.

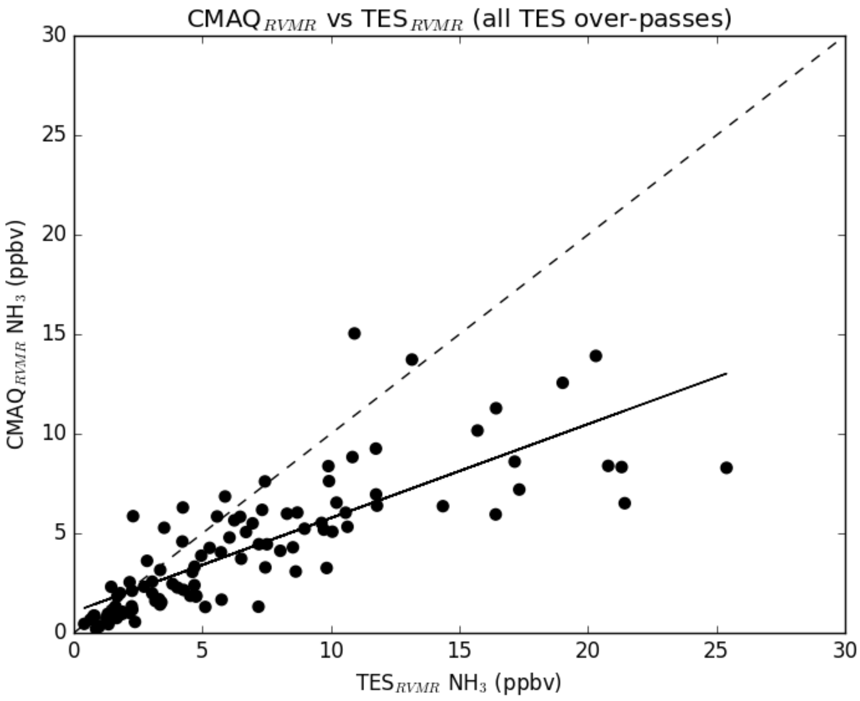

Figure 7. Scatter plot of $CMAQ_{base}$ and TES $NH_3$ representative volume mixing ratios for four TES special observation passes ($TES_{RVMR}$) during the CalNex campaign with statistics discussed in Table 3.

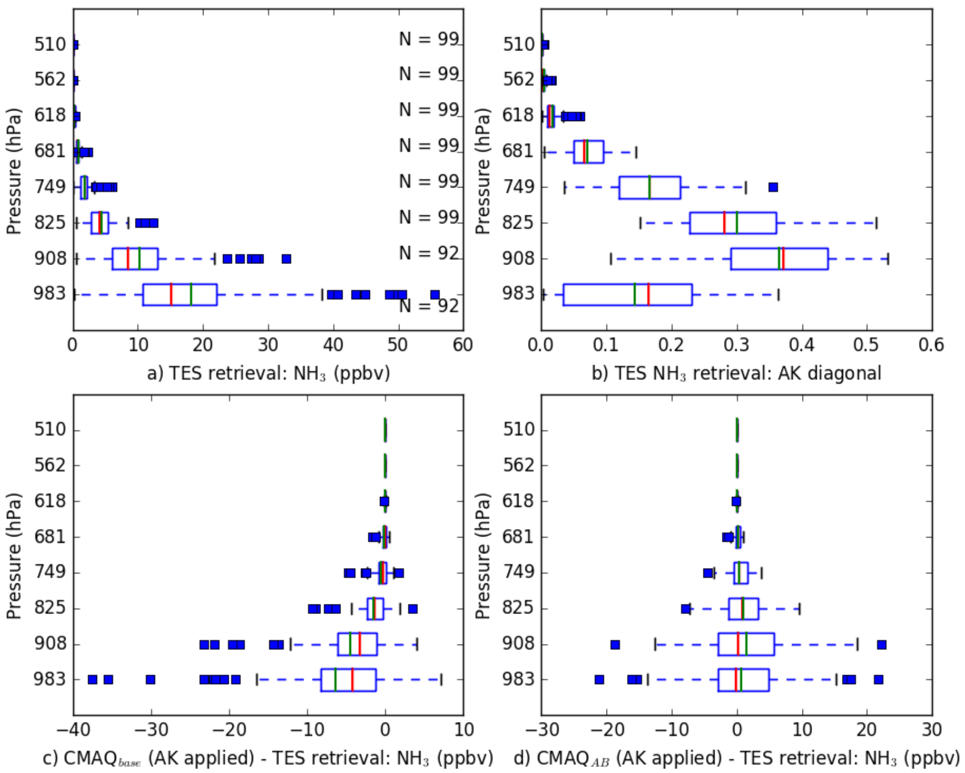

Figure 8. Boxplots of a) TES $NH_3$ retrieval by pressure level, b) TES $NH_3$ retrieval averaging kernel (AK) diagonal, c) difference between the TES $NH_3$ retrieval and $CMAQ_{base}$ modelled $NH_3$ interpolated to TES levels with an AK applied for the baseline model run and d) same as c) but for the $CMAQ_{AB}$ run. Box plots show the mean (green), median (red), interquartile range (IQR, blue box), whiskers at 1.5 IQR and outliers beyond that.

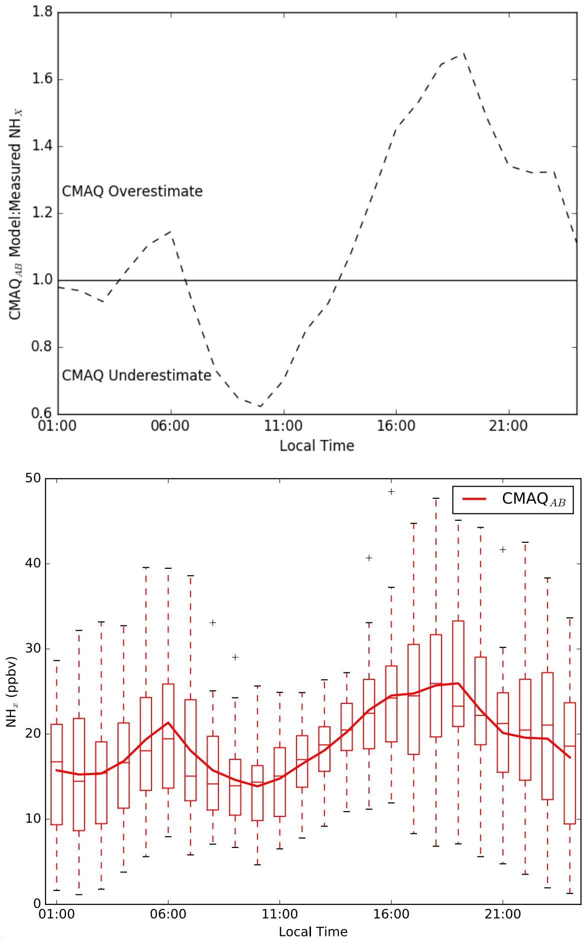

Figure 9. a) The average hourly ratio of CMAQ$_{AB}$ modelled to measured NH$_x$ (dashed line) mixing ratios at the Bakersfield ground site b) Boxplot of average hourly CMAQ$_{AB}$ modelled (red) NH$_x$ mixing ratios for the Bakersfield ground site.

Unknown
**Formatted:** Font:Bold